

DOI:10.1002/ejic.201201528

# Luminescent Pt–Ag Clusters Based on Neutral Benzoquinolate Cyclometalated Platinum Complexes

Antonio Martín,<sup>\*[a]</sup> Úrsula Belío,<sup>[a]</sup> Sara Fuertes,<sup>[a]</sup> and Violeta Sicilia<sup>[b]</sup>

*Dedicated to Professor Juan Forniés on the occasion of his 65th birthday*

**Keywords:** Donor–acceptor systems / Heterometallic complexes / Cluster compounds / Silver / Platinum / Luminescence / Metal–metal interactions / Pi interactions / Density functional calculations

Complexes of the type  $[\text{Pt}(\text{C}_6\text{F}_5)(\text{bzq})\text{L}]$  [ $\text{bzq}$  = 7,8-benzoquinolate;  $\text{L}$  =  $\text{PPh}_3$  (**2**), 2,6-diphenylpyridine ( $\text{pyPh}_2$ , **3**), tetrahydrothiophene (tth, **4**), MeCN (**5**)] were prepared by replacing the acetone ligand in  $[\text{Pt}(\text{C}_6\text{F}_5)(\text{bzq})(\text{Me}_2\text{CO})]$  (**1**) with the corresponding  $\text{L}$  ligand. The structures of complexes **2–4** were established by X-ray diffraction. Despite their neutral nature, complexes **1–5** react with  $\text{AgClO}_4$  in a 2:1 molar ratio to give the corresponding trinuclear complexes  $[\{\text{Pt}(\text{C}_6\text{F}_5)(\text{bzq})\text{L}\}_2\text{Ag}]\text{ClO}_4$  [ $\text{L}$  =  $\text{Me}_2\text{CO}$  (**6**),  $\text{PPh}_3$  (**7**),  $\text{pyPh}_2$  (**8**), tth (**9**), MeCN (**10**)], which contain Pt→Ag dative bonds. The structures of complexes **7**, **9**, and **10** were established by X-ray diffraction, which confirmed the existence of Pt–Ag bonds (ca. 2.8 Å) and short  $\eta^1$  bonding Ag–C interactions with the  $\text{C}_{\text{ipso}}$  atom of  $\text{bzq}$  (ca. 2.4 Å). Moreover, complexes **3**, **4**, **7**, **9**, and **10** show intermolecular  $\pi\cdots\pi$  interactions between the aromatic rings of the  $\text{bzq}$  ligands (separations of ca. 3.5 Å). The reactions of **1–5** with  $[\text{Ag}(\text{PPh}_3)(\text{OClO}_3)]$  in a 1:1 molar ratio proceed with interchange of the ligands between the metals and the formation of  $[\{\text{Pt}(\text{bzq})(\text{C}_6\text{F}_5)(\text{PPh}_3)\}_2\text{Ag}]\text{ClO}_4$  (**7**) and  $[\text{AgL}_2]\text{ClO}_4$  (X-ray). Only in the case

of  $\text{L} = \text{pyPh}_2$  (**3**) was the dinuclear complex  $[(\text{C}_6\text{F}_5)(\text{bzq})(\text{PPh}_3)\text{PtAg}(\text{pyPh}_2)]\text{ClO}_4$  (**11**) identified, and its structure was determined by X-ray diffraction. Complex **11** contains a Pt→Ag [2.8147(1) Å] bond and a  $\eta^1\text{-Ag-C}_{\text{ipso}}(\text{bzq})$  interaction [2.293(1) Å]. The electronic absorption and luminescence behaviors of **1–11** were investigated. The lower-lying absorption bands of the mononuclear complexes are ascribed to ligand-centered [ $^1\text{IL}$ ,  $\pi\text{-}\pi^*$  ( $\text{bzq}$ )] character mixed with some metal-to-ligand charge transfer [ $^1\text{MLCT}$   $5\text{d}(\text{Pt})\rightarrow\pi^*(\text{bzq})$ ]. For the trinuclear complexes, these bands are assigned to  $^1\text{ILCT}/^1\text{MM}'\text{LCT}$  [ $\pi\text{-}\pi^*(\text{bzq})/(\text{d}/\text{s}(\text{Pt},\text{Ag}))\rightarrow\pi^*(\text{bzq})$ ] transitions and to mixed  $^1\text{MLCT}/^1\text{L}'\text{LCT}$  [ $\text{MLCT}$   $5\text{d}(\text{Pt})\rightarrow\pi^*(\text{bzq})/[\text{L}'\text{LCT}, \text{Ar}_i\rightarrow\text{bzq}]$ ] for dinuclear complex **11** on the basis of time-dependent TD (DFT) calculations carried out on **2**, **4**, **5**, **9**, **10**, and **11Me** in  $\text{CH}_2\text{Cl}_2$ . Only **2** and the heteronuclear compounds are emissive in the solid state at room temperature; however, all of the complexes are emissive at 77 K (solids and glasses). In each case, the main phosphorescent emission seems to be due to a transition similar in character to the lowest-energy electronic absorption.

## Introduction

Metallophilic interactions between closed- or pseudo-closed-shell transition metals ( $\text{d}^{10}$ ,  $\text{d}^8$ ,  $\text{d}^{10}\text{s}^2$ ) is a field of great interest in inorganic chemistry.<sup>[1–12]</sup> In this respect, square-planar complexes of  $\text{Pt}^{\text{II}}$  are particularly well-suited systems that have allowed a huge variety of heteropolymet-

allic complexes involving  $\text{Pt}^{\text{II}}(\text{d}^8)\rightarrow\text{M}$  dative bonds, for which the acidic  $\text{M}$  center is  $\text{Cu}^{\text{I}}$ ,  $\text{Ag}^{\text{I}}$ ,  $\text{Au}^{\text{I}}$ ,  $\text{Cd}^{\text{II}}$ ,  $\text{Hg}^{\text{II}}$ ,  $\text{Tl}^{\text{I}}$ ,  $\text{Sn}^{\text{II}}$ , and  $\text{Pb}^{\text{II}}$ , to be prepared.<sup>[5,13–32]</sup>

These metal–metal bonds can be used as a tool in molecular or crystal engineering, as they act as a sort of link between different subassemblies. Thus, a wide array of interesting structural types with different nuclearities has been reported, from simple linear bimetallic compounds to infinite 1D chains.<sup>[15–19,22–24,30,32–39]</sup> Among other interesting properties, some complexes containing Pt–Ag bonds have been shown to exhibit interesting photophysical and photochemical properties,<sup>[1–10,18,31,39–53]</sup> which in some cases have been exclusively attributed to the presence of metallophilic bonds.

In the course of our current research, we developed synthetic methods for the preparation of complexes containing Pt–M bonds, mainly on the basis of the use of perhalo-

[a] Instituto de Síntesis Química y Catálisis Homogénea (ISQCH), CSIC – Universidad de Zaragoza, Departamento de Química Inorgánica, Facultad de Ciencias, 50009 Zaragoza, Spain  
Homepage: <http://organomet.unizar.es/platinum/personal/antoniomartin>

[b] Instituto de Síntesis Química y Catálisis Homogénea (ISQCH), CSIC – Universidad de Zaragoza, Departamento de Química Inorgánica, Escuela de Ingeniería y Arquitectura de Zaragoza, Campus Río Ebro, Edificio Torres Quevedo, 50018 Zaragoza, Spain

Supporting information for this article is available on the WWW under <http://dx.doi.org/10.1002/ejic.201201528>.

phenyl platinate(II) complexes.<sup>[13,16,17,34,37,38,54–57]</sup> We expanded this work with the simultaneous use of strong ligand-field cyclometalated C<sup>N</sup> ligands, such as 7,8-benzoquinolate (bzq).<sup>[16,17,39,53]</sup> This strong ligand field causes the  $d_{z^2}$  platinum orbital to raise its energy to favor the formation of stronger Pt→M dative bonds.<sup>[58,59]</sup> Thus, we have reported that the anionic [Pt(bzq)(C<sub>6</sub>X<sub>5</sub>)<sub>2</sub>]<sup>−</sup> (X = F, Cl) complex is a suitable starting material for the preparation of complexes with unsupported Pt–M bonds.<sup>[16,17,39]</sup> Depending on the reaction conditions, the complexes obtained show different structural features: bimetallic Pt–M [Pt(bzq)(C<sub>6</sub>X<sub>5</sub>)<sub>2</sub>]ML<sup>n+</sup> [M = Cd, L = cyclen, X = F,  $n = 1$ ;<sup>[16]</sup> M = Ag, L = PPh<sub>3</sub>, X = F or Cl,  $n = 0$ ;<sup>[17,39]</sup> M = Ag, L = tetrahydrothiophene (tht), X = F,  $n = 0$ ;<sup>[17,39]</sup>], trimetallic “sandwich” Pt–Ag–Pt [Pt(bzq)(C<sub>6</sub>F<sub>5</sub>)<sub>2</sub>]<sub>2</sub>Ag]<sup>−</sup>,<sup>[17]</sup> or the polymer metallic chain system ∙∙Pt–Ag–Pt–Ag–Pt∙∙[Pt(bzq)(C<sub>6</sub>F<sub>5</sub>)<sub>2</sub>]<sub>x</sub>Ag]<sup>−</sup>.<sup>[39]</sup> All the Pt–Ag complexes, in addition to containing intermetallic bonds, also contain very unusual  $\eta^1$  bonding interactions between the silver(I) center and the C<sub>ipso</sub> atom of the bzq ligand and are additionally stabilized by short or long-range  $\pi\cdots\pi$  stacking interactions between the aromatic rings of the bzq ligands.

All of these complexes exhibited interesting photoluminescent properties. For the [Pt(bzq)(C<sub>6</sub>F<sub>5</sub>)<sub>2</sub>Ag(L)] complexes (and also for [Pt(bzq)(C<sub>6</sub>F<sub>5</sub>)<sub>2</sub>Ag]<sub>x</sub> upon dissolution in donor solvents such as acetone or THF), the formation of the Pt–Ag bond results in a significant blueshift in the lowest-lying absorption relative to that of the [Pt(bzq)(C<sub>6</sub>X<sub>5</sub>)<sub>2</sub>]<sup>−</sup> starting material. This fact has been attributed to the stabilization and modification of the nature of the HOMO, which changes the character of the transition from intraligand/metal-to-ligand charge transfer (<sup>1</sup>IL/<sup>1</sup>MLCT) in [Pt(bzq)(C<sub>6</sub>F<sub>5</sub>)<sub>2</sub>]<sup>−</sup> to the admixture ligand-to-ligand/metal-to-ligand charge transfer (<sup>1</sup>L/<sup>1</sup>LCT/<sup>1</sup>MLCT) in the bimetallic fragments. The emission in [Pt(bzq)(C<sub>6</sub>F<sub>5</sub>)<sub>2</sub>Ag(L)] is also mainly associated with an admixture of <sup>3</sup>MLCT/<sup>3</sup>L/<sup>1</sup>LCT, which is only slightly modified by the Ag center. By contrast, both the experimental data in the solid state and the theoretical calculations on “[Pt(bzq)(C<sub>6</sub>F<sub>5</sub>)<sub>2</sub>Ag]<sup>−</sup>” as a model for [Pt(bzq)(C<sub>6</sub>F<sub>5</sub>)<sub>2</sub>Ag]<sub>x</sub> suggest that excitation of the polymer moves the electron density from the platinum fragments; the C<sub>6</sub>F<sub>5</sub> rings have a remarkable contribution to an orbital with strong Pt and Ag metallic character. Absorption and emission of the polymer in the solid state is therefore suggested to be associated with an electronic transition of a mixed [Pt(bzq)→Ag]/[Ar<sub>r</sub>→Ag] character. For the trimetallic [Pt(bzq)(C<sub>6</sub>F<sub>5</sub>)<sub>2</sub>]<sub>2</sub>Ag]<sup>−</sup> complex, two different polymorphs were obtained from acetone/*n*-hexane, and they exhibited visibly different luminescence at room temperature. The crystal structures of both anions are different, not only in their form, with a different conformation of the platinum planes, but also in terms of packing.

In this paper we continue our study on these kinds of complexes by exploring the ability of the [Pt(bzq)(C<sub>6</sub>F<sub>5</sub>)<sub>2</sub>]<sup>−</sup> {L = Me<sub>2</sub>CO, PPh<sub>3</sub>, 2,6-diphenylpyridine (pyPh<sub>2</sub>), tht, MeCN} starting materials to form new complexes of diverse nuclearity containing Pt–Ag bonds. In principle, the

neutral [Pt(bzq)(C<sub>6</sub>F<sub>5</sub>)(L)] complexes have a disadvantage with respect to the previously used [Pt(bzq)(C<sub>6</sub>X<sub>5</sub>)<sub>2</sub>]<sup>−</sup> complex, as the anionic nature of this latter complex should increase the electron density on the Pt center to thus favor the formation of the Pt→Ag dative bond.<sup>[13]</sup> Nevertheless, there are examples of neutral platinum complexes that have been used as starting materials in the preparation of Pt→Ag dative bonds with success.<sup>[32,53]</sup> Thus, after the preparation of the corresponding [Pt(bzq)(C<sub>6</sub>F<sub>5</sub>)(L)] starting materials, we have achieved the preparation of several trimetallic Pt–Ag–Pt and one bimetallic Pt–Ag complexes, which were characterized and studied by X-ray crystallography and NMR spectroscopy. Finally, their optical properties were investigated and time-dependent density functional theory (TD-DFT) calculations were performed to gain better insight into the nature of the electronic transitions.

## Results and Discussion

### Synthesis and Characterization of Cyclometalated [Pt(C<sub>6</sub>F<sub>5</sub>)(bzq)L] {L = PPh<sub>3</sub> (2), pyPh<sub>2</sub> (3), tht (4), MeCN (5)}

The [Pt(C<sub>6</sub>F<sub>5</sub>)(bzq)(Me<sub>2</sub>CO)] (1) complex is a suitable precursor for the preparation of [Pt(C<sub>6</sub>F<sub>5</sub>)(bzq)L] complexes because the acetone group is easily replaced by other L ligands.<sup>[60]</sup> Thus, the addition of equimolar amounts of PPh<sub>3</sub>, pyPh<sub>2</sub>, and tht to separate acetone solutions of **1** at 0 °C under a protective Ar atmosphere allowed the corresponding [Pt(C<sub>6</sub>F<sub>5</sub>)(bzq)L] {L = PPh<sub>3</sub> (2), pyPh<sub>2</sub> (3), tht (4)} complexes to be obtained as yellow solids that precipitated after partial evaporation of the solvent. The [Pt(C<sub>6</sub>F<sub>5</sub>)(bzq)(MeCN)] (5) complex was obtained by dissolving **1** in acetonitrile under the same conditions. After 2 min of stirring, the solvent was removed to dryness under vacuum, and the resulting yellow solid was identified as **5** (see the Exp. Sect.).

The IR spectra of complexes **2–5** confirm the replacement of acetone in **1**, as the  $\nu_{\text{CO}}$  vibration band at 1669 cm<sup>−1</sup> is absent, and the bands corresponding to the coordination ligands incorporated into the coordination sphere of the Pt atoms are now present (see the Exp. Sect.). The <sup>1</sup>H NMR spectra of these complexes also show signals due to the new ligands, besides the ones that can be attributed to the bzq ligand with the expected relative intensity. The <sup>19</sup>F NMR spectra of **2–5** present the same pattern of three signals corresponding to the pentafluorophenyl ligand. The two *ortho*-F atoms cause one downfield signal with platinum satellites. At higher field, one signal for the *meta*-F atom and one for the *para*-F atom can be observed. For **2**, the <sup>31</sup>P NMR spectrum shows a singlet with platinum satellites attributable to the phosphorus atom of the PPh<sub>3</sub> ligand. All the NMR details are compiled in the Exp. Sect.

The structures of complexes **2**, **4**, and **5** were established by X-ray diffraction studies. Figures 1, 2, and 3 show views of the corresponding complexes, and Tables 1, 2, and 3 list a selection of relevant bond lengths and angles. All three complexes are square-planar complexes, and the bzq ligand is coplanar to the metal plane. The pentafluorophenyl ligand is in a *trans* position with respect to the nitrogen atom of the bzq ligand. As was previously observed in other platinum(II) complexes containing the bzq ligand, the complexes establish a supramolecular arrangement through  $\pi\cdots\pi$  interactions of the bzq aromatic ring system of different moieties, which stack in a parallel, head-to-tail fash-

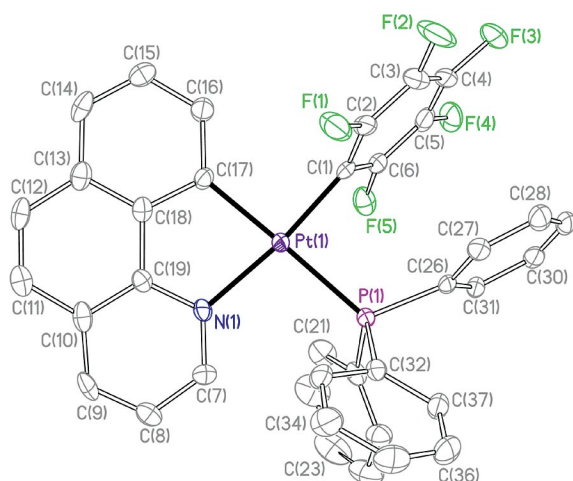


Figure 1. View of the molecular structure of  $[\text{Pt}(\text{C}_6\text{F}_5)(\text{bzq})(\text{PPh}_3)]$  (**2**).

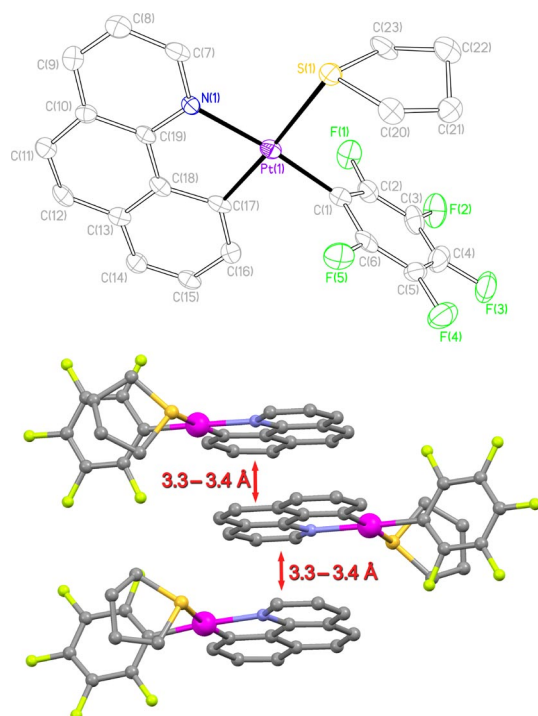


Figure 2. Top: view of the molecular structure of  $[\text{Pt}(\text{C}_6\text{F}_5)(\text{bzq})(\text{tht})]$  (**4**). Bottom: supramolecular arrangement of the three units showing the  $\pi\cdots\pi$  stacking.

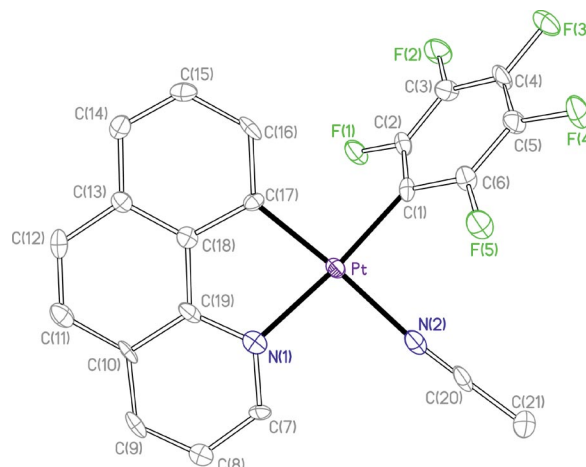


Figure 3. View of the molecular structure of  $[\text{Pt}(\text{C}_6\text{F}_5)(\text{bzq})(\text{MeCN})]$  (**5**).

Table 1. Selected bond lengths and angles for  $[\text{Pt}(\text{C}_6\text{F}_5)(\text{bzq})(\text{PPh}_3)] \cdot 0.2\text{Me}_2\text{CO}$  (**2**·0.2Me<sub>2</sub>CO).

Bond length [Å]			
Pt(1)–C(1)	2.015(6)	Pt(1)–C(17)	2.041(6)
Pt(1)–N(1)	2.107(5)	Pt(1)–P(1)	2.3224(16)
Bond angle [°]			
C(1)–Pt(1)–C(17)	92.5(2)	C(1)–Pt(1)–N(1)	172.7(2)
C(17)–Pt(1)–N(1)	80.6(2)	C(1)–Pt(1)–P(1)	89.36(17)
C(17)–Pt(1)–P(1)	176.16(19)	N(1)–Pt(1)–P(1)	97.70(15)

Table 2. Selected bond lengths and angles for  $[\text{Pt}(\text{C}_6\text{F}_5)(\text{bzq})(\text{tht})] \cdot 2/3\text{CH}_2\text{Cl}_2$  (**4**·2/3CH<sub>2</sub>Cl<sub>2</sub>).

Bond length [Å]			
Pt(1)–C(17)	2.000(7)	Pt(1)–C(1)	2.003(8)
Pt(1)–N(1)	2.078(7)	Pt(1)–S(1)	2.3719(19)
Bond angle [°]			
C(17)–Pt(1)–C(1)	91.8(3)	C(17)–Pt(1)–N(1)	82.1(3)
C(1)–Pt(1)–N(1)	173.9(3)	C(17)–Pt(1)–S(1)	176.1(2)
C(1)–Pt(1)–S(1)	92.1(2)	N(1)–Pt(1)–S(1)	93.98(19)

Table 3. Selected bond lengths and angles for  $[\text{Pt}(\text{C}_6\text{F}_5)(\text{bzq})(\text{MeCN})]$  (**5**).

Bond length [Å]			
Pt–C(17)	1.993(7)	Pt–C(1)	2.016(8)
Pt–N(2)	2.070(7)	Pt–N(1)	2.085(7)
Bond angle [°]			
C(17)–Pt–C(1)	93.6(3)	C(17)–Pt–N(2)	175.5(3)
C(1)–Pt–N(2)	90.3(3)	C(17)–Pt–N(1)	81.6(3)
C(1)–Pt–N(1)	173.9(3)	N(2)–Pt–N(1)	94.6(3)

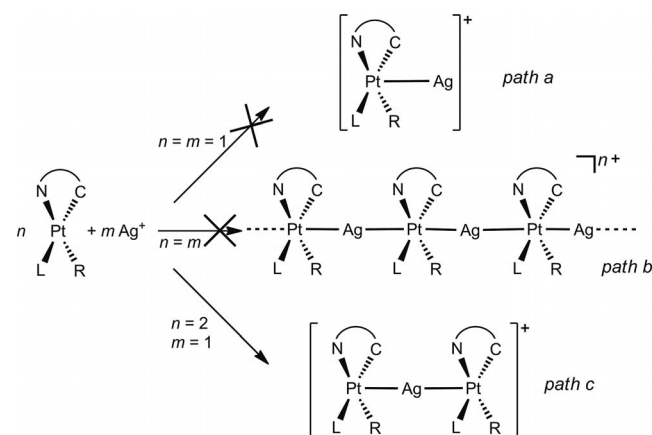
ion. Thus, in **2** four units of the  $[\text{Pt}(\text{C}_6\text{F}_5)(\text{bzq})(\text{PPh}_3)]$  complex are stacked (Figure S1, Supporting Information) with interplanar bzq distances of ca. 3.4 Å, whereas in **4** the asymmetric unit contains three stacked units of the  $[\text{Pt}(\text{C}_6\text{F}_5)(\text{bzq})(\text{tht})]$  complex (Figure 2, bottom) with interplanar bzq distances of ca. 3.3–3.4 Å. No other  $\pi\cdots\pi$  interactions are observed among these groups of four or three

units and other adjacent moieties. In contrast, in **5** an infinite array of stacked  $[\text{Pt}(\text{C}_6\text{F}_5)(\text{bzq})(\text{MeCN})]$  units is found with similar interplanar bzq distances (Figure S2, Supporting Information). This kind of supramolecular arrangement has been found in other complexes with the bzq ligand<sup>[17,18,39,53,60,61]</sup> and in other cyclometalated planar ligands.<sup>[32,62]</sup> Along with H-bonding, this kind of  $\pi\cdots\pi$  stacking is one of the most important secondary interactions<sup>[63–68]</sup> in the field of modern supramolecular chemistry,<sup>[69–72]</sup> as it plays an important role in processes such as molecular self-assembly and self-recognition of aromatic entities in the crystal state.

### Reactivity of 1–5 towards $\text{AgClO}_4$ : Synthesis and Characterization of $\{[\text{Pt}(\text{C}_6\text{F}_5)(\text{bzq})\text{L}]_2\text{Ag}\}\text{ClO}_4$ $\{\text{L} = \text{Me}_2\text{CO}$ (**6**), $\text{PPh}_3$ (**7**), $\text{pyPh}_2$ (**8**), $\text{tht}$ (**9**), $\text{MeCN}$ (**10**)

Complexes **1–5** were treated with  $\text{AgClO}_4$  with the aim to prepare heterometallic complexes containing  $\text{Pt}\rightarrow\text{Ag}$  dative bonds. As mentioned above, it was previously reported that anionic  $\text{Pt}^{\text{II}}$  precursors favor the obtaining of such  $\text{Pt}\rightarrow\text{M}$  complexes, because the additional electron density borne by the platinum center can be donated to the acidic center.<sup>[13]</sup> Hence, despite the fact that some neutral  $\text{Pt}^{\text{II}}$  precursors have been used,<sup>[32,53]</sup> the greatest success in the preparation of complexes with  $\text{Pt}\rightarrow\text{M}$  donor–acceptor bonds was achieved with anionic  $\text{Pt}^{\text{II}}$  complexes as starting materials.

In any case, we investigated the reactivities of **1–5** towards  $\text{AgClO}_4$  in molar ratios of 1:1 and 2:1. The 1:1 molar ratio could lead to the preparation of discrete dinuclear  $[\text{Pt}–\text{Ag}]^+$  complexes (Scheme 1, a) and polymeric infinite  $[\cdots\text{Pt}–\text{Ag}–\text{Pt}–\text{Ag}–\text{Pt}\cdots]^{n+}$  species (Scheme 1, b), whereas the 2:1 molar ratio led to trinuclear  $[\text{Pt}–\text{Ag}–\text{Pt}]^+$  “sandwiches” (Scheme 1, c).



Scheme 1.

Thus, the reactions of complexes **1–5** with  $\text{AgClO}_4$  in a 2:1 molar ratio were carried out in acetone at  $0^\circ\text{C}$  under an Ar atmosphere in the absence of light for 30 min. After workup of the reaction mixtures, compounds  $\{[\text{Pt}(\text{C}_6\text{F}_5)(\text{bzq})\text{L}]_2\text{Ag}\}\text{ClO}_4$   $\{\text{L} = \text{Me}_2\text{CO}$  (**6**),  $\text{PPh}_3$  (**7**),  $\text{pyPh}_2$  (**8**),  $\text{tht}$  (**9**),  $\text{MeCN}$  (**10**) were obtained as yellow

solids; their structures were elucidated through analytical and spectroscopic data (see the Exp. Sect.). When the reactions are carried out under the same experimental conditions but in a 1:1 molar ratio, only oily residues were obtained, which were identified as mixtures of **6–10** and unreacted  $\text{AgClO}_4$ .

These results indicate that only the trinuclear complexes (Scheme 1, c) could be isolated. The stabilities of the trinuclear complexes relative to those of the complexes that could be obtained by using a 1:1 molar ratio can be rationalized by the neutral character of starting  $\text{Pt}^{\text{II}}$  products **1–5**. These complexes would not have enough electron density on their basic metal  $\text{Pt}^{\text{II}}$  center to satisfy the requirement of one acidic silver center, but two  $\text{Pt}^{\text{II}}$  centers have to cooperate to stabilize the trinuclear complex with the formation of two  $\text{Pt}\rightarrow\text{Ag}$  bonds with the same  $\text{Ag}^{\text{I}}$  center. Notably, as mentioned above, the  $[(\text{C}_6\text{F}_5)_2(\text{bzq})\text{PtAg}]_x$  complex,<sup>[39]</sup> which is similar to the one that would result from the path depicted in Scheme 1 (b) does exist. In that case, the starting material is an anionic  $\text{Pt}^{\text{II}}$  complex (i.e.,  $[\text{Pt}(\text{C}_6\text{F}_5)_2(\text{bzq})]^-$ ), and thus, the  $\text{Pt}^{\text{II}}$  center seems to be more able to fulfil the electron necessities of the silver center.

The IR spectra of complexes **6–10** show the presence of two signals assignable to the  $\text{ClO}_4$  anion: one sharp band at  $621\text{ cm}^{-1}$  and another broad band at  $1095\text{ cm}^{-1}$ . Moreover, the expected signals caused by bzq and the corresponding L ligand can be found.

The  $^1\text{H}$  NMR spectra of complexes **6–10** show signals corresponding to the L ligands, in addition to the ones attributed to the bzq ligand with the expected relative intensity. The  $^{19}\text{F}$  NMR spectra of **6–10** present only one set of signals, which is indicative of the equivalence of the pentafluorophenyl groups of the two “ $\text{Pt}(\text{C}_6\text{F}_5)(\text{bzq})\text{L}$ ” subunits. The pattern of the signals is similar to the one described above for complexes **2–5**. Finally, for **7** the  $^{31}\text{P}$  NMR spectrum shows a singlet signal with platinum satellites attributable to the phosphorus atom of the  $\text{PPh}_3$  ligand. Details of the NMR spectroscopic data are compiled in the Exp. Sect.

### Crystal Structures of $\{[\text{Pt}(\text{C}_6\text{F}_5)(\text{bzq})\text{L}]_2\text{Ag}\}\text{ClO}_4$ $\{\text{L} = \text{PPh}_3$ (**7**), $\text{tht}$ (**9**), $\text{MeCN}$ (**10**)

The structures of complexes **7**, **9**, and **10** were established by X-ray diffraction studies. Figures 4, 5, and 6 show views of the corresponding complexes, and Tables 4, 5, and 6 list a selection of relevant bond lengths and angles.

Determination of the crystal structures confirmed that, in the solid state, these complexes are trinuclear with a “sandwich” disposition. The two “ $\text{Pt}(\text{C}_6\text{F}_5)(\text{bzq})\text{L}$ ” fragments are linked to the silver center through  $\text{Pt}\rightarrow\text{Ag}$  donor–acceptor bonds. The  $\text{Pt}–\text{Ag}$  distances are  $2.823(1)$  and  $2.745(1)\text{ \AA}$  for **7**,  $2.835(1)$  and  $2.841(1)\text{ \AA}$  for **9**, and  $2.792(1)$  and  $2.765(1)\text{ \AA}$  for **10**. These distances are in the range found for other complexes containing  $\text{Pt}\rightarrow\text{Ag}$  bonds,<sup>[13,17,23,24,32,34,35,39,54,73–79]</sup> The structures of **7**, **9**, and **10** can be compared with the ones described for the two polymorphs of the analogous  $(\text{NBu}_4)[\{\text{Pt}(\text{C}_6\text{F}_5)_2(\text{bzq})\}_2\text{Ag}]$

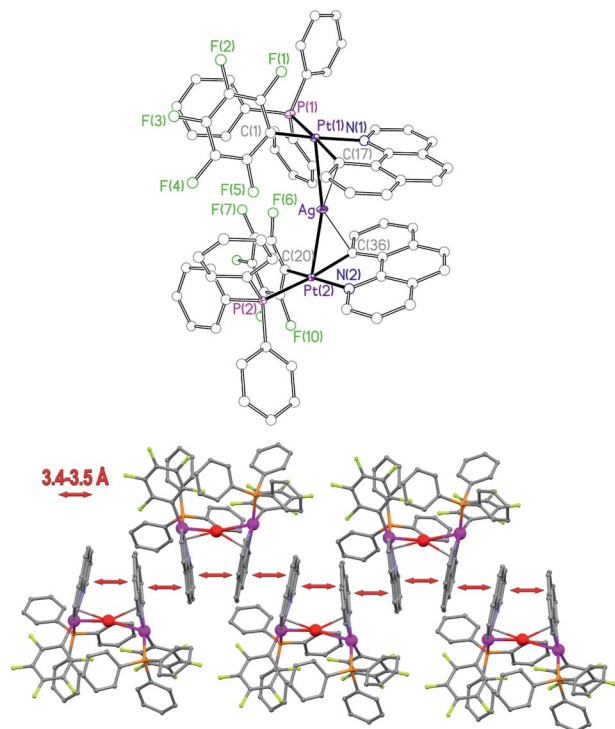


Figure 4. Top: view of the molecular structure of the cation of  $[\{\text{Pt}(\text{C}_6\text{F}_5)(\text{bzq})(\text{PPh}_3)_2\text{Ag}\}]\text{ClO}_4$  (**7**). Bottom: supramolecular arrangement of the infinite  $\pi\cdots\pi$  stacking array.

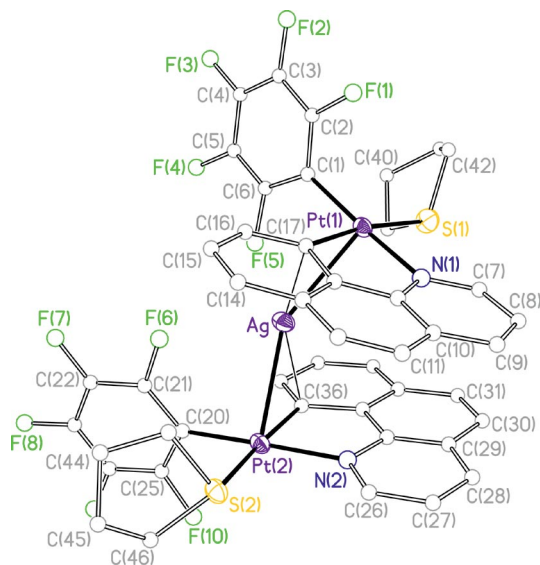


Figure 5. View of the molecular structure of the cation of  $[\{\text{Pt}(\text{C}_6\text{F}_5)(\text{bzq})(\text{tht})_2\text{Ag}\}]\text{ClO}_4$  (**9**).

complex,<sup>[17]</sup> which is also a “sandwich”-type complex with a Pt–Ag–Pt bond system that is similar to that found in the complex described here. As mentioned above, the starting material for  $(\text{NBu}_4)[\{\text{Pt}(\text{C}_6\text{F}_5)_2(\text{bzq})\}_2\text{Ag}]$  is anionic, and the resulting trinuclear complex is also anionic. Thus, stronger Pt–Ag bonds and, hence, shorter Pt–Ag distances could be expected in  $(\text{NBu}_4)[\{\text{Pt}(\text{C}_6\text{F}_5)_2(\text{bzq})\}_2\text{Ag}]$ . The two polymorphs of this anionic “sandwich” show Pt–Ag

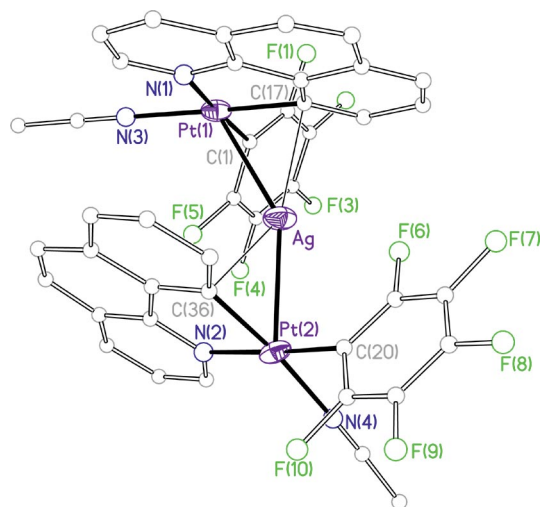


Figure 6. View of the molecular structure of the cation of  $[\{\text{Pt}(\text{C}_6\text{F}_5)(\text{bzq})(\text{MeCN})_2\text{Ag}\}]\text{ClO}_4$  (**10**).

Table 4. Selected bond lengths and angles for  $[\{\text{Pt}(\text{C}_6\text{F}_5)(\text{bzq})(\text{PPh}_3)_2\text{Ag}\}]\text{ClO}_4 \cdot \text{CH}_2\text{Cl}_2$  (**7**· $\text{CH}_2\text{Cl}_2$ ).

Bond length [Å]			
Pt(1)–C(1)	2.028(4)	Pt(1)–C(17)	2.062(4)
Pt(1)–N(1)	2.106(3)	Pt(1)–P(1)	2.3472(10)
Pt(1)–Ag	2.8225(3)	Pt(2)–C(20)	2.024(4)
Pt(2)–C(36)	2.071(4)	Pt(2)–N(2)	2.122(3)
Pt(2)–P(2)	2.3336(10)	Pt(2)–Ag	2.7447(3)
Ag–C(17)	2.351(4)	Ag–C(36)	2.460(3)
Bond angle [°]			
C(1)–Pt(1)–C(17)	90.64(15)	C(1)–Pt(1)–N(1)	168.49(13)
C(17)–Pt(1)–N(1)	80.36(14)	C(1)–Pt(1)–P(1)	91.30(10)
C(17)–Pt(1)–P(1)	176.22(10)	N(1)–Pt(1)–P(1)	98.11(9)
C(20)–Pt(2)–C(36)	91.66(15)	C(20)–Pt(2)–N(2)	168.58(13)
C(36)–Pt(2)–N(2)	80.29(13)	C(20)–Pt(2)–P(2)	89.74(11)
C(36)–Pt(2)–P(2)	173.72(10)	N(2)–Pt(2)–P(2)	99.14(9)
C(17)–Ag–C(36)	134.78(13)	Pt(2)–Ag–Pt(1)	161.994(13)

Table 5. Selected bond lengths and angles for  $[\{\text{Pt}(\text{C}_6\text{F}_5)(\text{bzq})(\text{tht})_2\text{Ag}\}]\text{ClO}_4 \cdot 1.5\text{Me}_2\text{CO}$  (**9**· $1.5\text{Me}_2\text{CO}$ ).

Bond length [Å]			
Pt(1)–C(1)	2.001(5)	Pt(1)–C(17)	2.019(5)
Pt(1)–N(1)	2.081(5)	Pt(1)–S(1)	2.3685(14)
Pt(1)–Ag	2.8350(5)	Pt(2)–C(20)	2.002(5)
Pt(2)–C(36)	2.020(5)	Pt(2)–N(2)	2.092(5)
Pt(2)–S(2)	2.3686(14)	Pt(2)–Ag	2.8410(5)
Ag–C(17)	2.347(5)	Ag–C(36)	2.339(6)
Bond angle [°]			
C(1)–Pt(1)–C(17)	93.6(2)	C(1)–Pt(1)–N(1)	171.74(19)
C(17)–Pt(1)–N(1)	81.6(2)	C(1)–Pt(1)–S(1)	92.72(14)
C(17)–Pt(1)–S(1)	171.82(16)	N(1)–Pt(1)–S(1)	92.77(13)
C(20)–Pt(2)–C(36)	93.9(2)	C(20)–Pt(2)–N(2)	173.8(2)
C(36)–Pt(2)–N(2)	81.6(2)	C(20)–Pt(2)–S(2)	91.98(15)
C(36)–Pt(2)–S(2)	173.95(18)	N(2)–Pt(2)–S(2)	92.69(13)
C(36)–Ag–C(17)	154.1(2)	Pt(1)–Ag–Pt(2)	149.139(19)

distances of 2.758(1), 2.684(1), 2.702(1), and 2.690(1) Å, which, in general, are slightly shorter than the ones found in **7**, **9**, and **10**, but this difference can also be attributed to

Table 6. Selected bond lengths and angles for  $[\{\text{Pt}(\text{C}_6\text{F}_5)(\text{bzq})\text{-(NCMe)}\}_2\text{Ag}]\text{ClO}_4 \cdot 2.5\text{CH}_2\text{Cl}_2 \cdot 0.5n\text{-C}_6\text{H}_{14}$  (**10**·2.5CH<sub>2</sub>Cl<sub>2</sub>·0.5n-C<sub>6</sub>H<sub>14</sub>).

Bond length [Å]			
Pt(1)–C(17)	1.999(7)	Pt(1)–C(1)	2.029(8)
Pt(1)–N(3)	2.061(9)	Pt(1)–N(1)	2.072(7)
Pt(1)–Ag	2.7924(8)	Pt(2)–C(20)	2.013(10)
Pt(2)–C(36)	2.006(7)	Pt(2)–N(4)	2.063(7)
Pt(2)–N(2)	2.096(7)	Pt(2)–Ag	2.7646(8)
Ag–C(17)	2.425(8)	Ag–C(36)	2.467(8)
Bond angle [°]			
C(17)–Pt(1)–C(1)	93.7(3)	C(17)–Pt(1)–N(3)	175.3(3)
C(1)–Pt(1)–N(3)	90.9(3)	C(17)–Pt(1)–N(1)	83.1(3)
C(1)–Pt(1)–N(1)	176.8(3)	N(3)–Pt(1)–N(1)	92.2(3)
C(20)–Pt(2)–C(36)	93.2(3)	C(20)–Pt(2)–N(4)	90.0(3)
C(36)–Pt(2)–N(4)	174.4(3)	C(20)–Pt(2)–N(2)	175.1(3)
C(36)–Pt(2)–N(2)	81.9(2)	N(4)–Pt(2)–N(2)	94.8(3)
C(17)–Ag–C(36)	136.59(19)	Pt(2)–Ag–Pt(1)	147.79(3)

steric factors caused by the disposition of the ligands in the complexes or to intermolecular packing forces.<sup>[80]</sup>

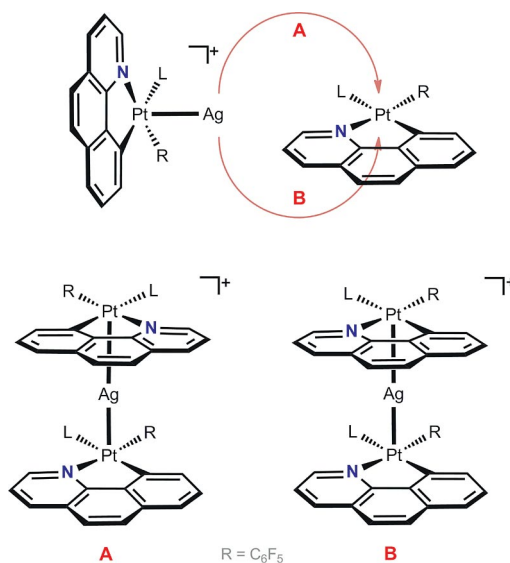
Besides the Pt–Ag bonds, in complexes **7**, **9**, and **10** the silver center also establishes a short  $\eta^1$  interaction with the  $C_{\text{ipso}}$  atom of the bzq ligands [C(17) and C(36) in Figures 4–6] with Ag–C distances of 2.351(4) and 2.460(3) Å for **7**, 2.347(8) and 2.339(8) Å for **9**, and 2.425(8) and 2.467(8) Å for **10**. These  $\eta^1$ -Ag–C contacts were previously found in other “(bzq)Pt → Ag”<sup>[17,39]</sup> and “(L)Pt → Ag” complexes, in which L is another aromatic planar cyclometalated ligand similar to bzq, such as 2-phenylpyridinate, 2-(2-tyenyl)pyridinate,<sup>[23]</sup> or ethyl 2,6-diphenylisonicotinate.<sup>[32]</sup> These  $\eta^1$ -Ag–C interactions are important and, along the Pt → Ag bonds, contribute to fulfil the electron density requirements of the acidic silver center. The affinity of this metal for some  $\pi$ -donor systems is well known,<sup>[33,69–72,81–89]</sup> and the  $\eta^1$  and  $\eta^2$  coordination modes are most common. The Ag–C lines are usually perpendicular to the aromatic planar ring system, which is also more or less observed in **7**, **9**, and **10**, given the geometric limitations imposed by the Pt–Ag bonds. Thus, the angles between the Ag–C lines and the perpendicular to the best bzq planes are 15.5(1) and 20.3(1)° for **7**, 13.6(1) and 12.1(1)° for **9**, and 14.6(2) and 18.3(2)° for **10**.

In **7**, the silver center is located relatively close to one of the *ortho* fluorine atoms of each pentafluorophenyl group [Ag···F(5) 2.838(2) Å, Ag···F(6) 2.691(2) Å], whereas in **10** only one *o*-F is relatively near the Ag atom [Ag···F(6) 2.699(10) Å], and in **9**, the separation is longer [Ag···F(5) 2.914(5) Å, Ag···F(6) 2.898(4) Å]. These short distances are frequently found in pentafluorophenyl complexes and are considered as secondary contacts that also contribute to complete the electron donation to the acidic silver and, thus, to the final stabilization of the complex.<sup>[13]</sup>

The Pt–Ag–Pt angle is 161.99(1)° in **7**, 149.14(2)° in **9**, and 147.79(3)° in **10**. The Pt–Ag lines are not perpendicular to the square-planar environments of the Pt atoms; the angles to the perpendicular to these planes are 32.1(1)° for Pt(1) and 24.7(1)° for Pt(2) in **7**, 30.1(1)° for Pt(1) and

34.1(1)° for Pt(2) in **9**, and 32.4(2)° for Pt(1) and 32.6(2)° for Pt(2) in **10**. In principle, the best disposition for an optimal Pt → M occurs when the intermetallic line is perpendicular to the Pt square-plane, which maximizes overlap of the full  $5d_{z^2}$  Pt<sup>II</sup> orbital containing the electron pair donated to form the dative bond with the empty orbitals of the acidic metal center. Nevertheless, in these kinds of complexes there are some other factors that force the Pt–Ag bond to deviate from this ideal perpendicular disposition. Some of these factors are electronic, such as  $\eta^1$ -Ag–C interactions or *o*-F contacts, or steric resulting from the presence of bulky ligands, such as C<sub>6</sub>F<sub>5</sub> or PPh<sub>3</sub>, along with other less sterically demanding ligands, such as bzq, Me<sub>2</sub>CO, or MeCN.

In this line, complexes **7**, **9**, and **10** show substantial conformational differences in the relative dispositions of the two square-planar environments of each structure. In principle, two relative dispositions of the Pt planes are possible in these “sandwich” trinuclear complexes (see Scheme 2). In disposition **A**, the coordination of the two Pt centers takes place in such a way that the positions of the N and  $C_{\text{ipso}}$  atoms of each bzq ligand alternate, and thus, the relative positions of the L and C<sub>6</sub>F<sub>5</sub> ligands of each “Pt(C<sub>6</sub>F<sub>5</sub>)(bzq)L” fragment also alternate. In contrast, in disposition **B**, the relative positions of all the analogous atoms bonded to the Pt center in each “Pt(C<sub>6</sub>F<sub>5</sub>)(bzq)L” fragment coincide. These two conformations were previously found in similar complexes containing the bzq and C<sub>6</sub>F<sub>5</sub> ligands.<sup>[17,39]</sup> Moreover, it is necessary to take into consideration the possibility that the “Pt(C<sub>6</sub>F<sub>5</sub>)(bzq)L” fragments turn around the Pt–Ag bonds and the variability of the Pt–Ag–Pt angles (see above). For all these reasons, complexes **7**, **9**, and **10** {and (NBu<sub>4</sub>)[{Pt(C<sub>6</sub>F<sub>5</sub>)<sub>2</sub>(bzq)<sub>2</sub>Ag]<sup>[17]</sup>} are very flexible and are able to adapt their geometry to the electronic and steric demands mentioned above, as well as the crystal-packing effects.



Scheme 2.

Thus, in complex **7** the dihedral angle between the best Pt square-planes is 25.6(1)°, and these planes lean over one

another in such a way that the bzq ligands of the two sub-units are almost eclipsed [torsion angle N(1)–Pt(1)–Pt(2)–N(2) = 67.4(1)°] and adopt conformation A (Scheme 2). This disposition allows maximum separation between the phenyl groups of the two PPh<sub>3</sub> ligands, which are the bulkiest in this complex. Conformation A is also observed in **9**, with a dihedral angle of 24.4(1)° between the two Pt planes, but here, the two “Pt(C<sub>6</sub>F<sub>5</sub>)(bzq)(tbt)” fragments are rotated and the torsion angle N(1)–Pt(1)–Pt(2)–N(2) is only 15.4(1)°. In contrast, complex **10** shows conformation B, probably to allow maximum separation of the most sterically demanding ligands of the complex, in this case, the pentafluorophenyl groups.

Study of the supramolecular packing of complexes **7**, **9**, and **10** has shown an infinite array of cations connected through  $\pi\cdots\pi$  interactions of the planar aromatic rings of the bzq ligands, in a similar fashion to that described above for complexes **2**, **4**, and **5** and in other complexes previously reported.<sup>[17,18,32,39,53,60–62]</sup> The interplanar separations are close to 3.4 Å, and as an example, Figure 4 (bottom) shows a fragment of this array as found in complex **7**.

### Reactivities of 1–5 towards [Ag(PPh<sub>3</sub>)(OCIO<sub>3</sub>)]

As the reactions of complexes **1–5** with AgClO<sub>4</sub> did not result in dinuclear discrete complexes or polymeric infinite species containing Pt–Ag bonds, we tried another silver reagent: [Ag(PPh<sub>3</sub>)(OCIO<sub>3</sub>)]. In this complex, the silver center coordinates to a strong PPh<sub>3</sub> ligand, which blocks one of its possible coordination positions and contributes to fulfil the electronic requirements of the acidic silver. The aim was to prepare dinuclear [Pt(bzq)(C<sub>6</sub>F<sub>5</sub>)LAg(PPh<sub>3</sub>)ClO<sub>4</sub>] complexes containing a donor–acceptor Pt→Ag bond. This synthetic strategy is well known and has been used with positive results.<sup>[13,17,54,79]</sup>

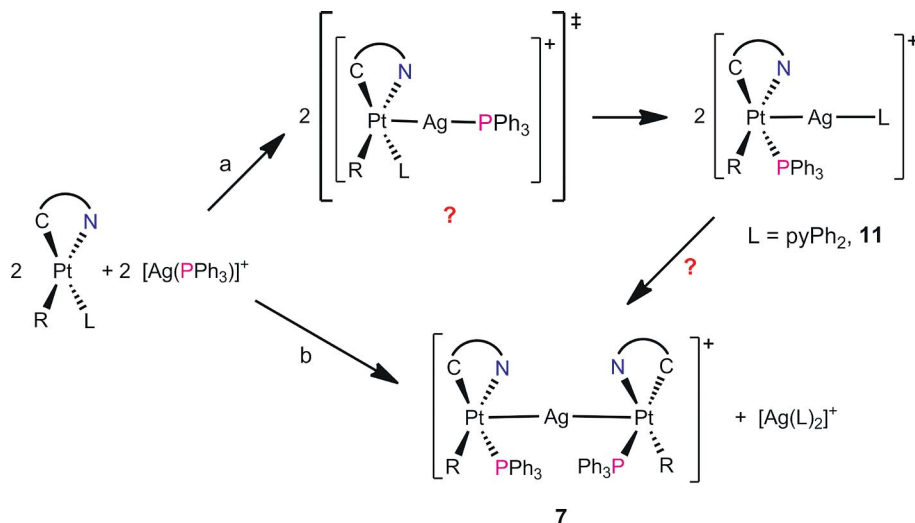
Thus, complexes **1–5** were treated with [Ag(PPh<sub>3</sub>)(OCIO<sub>3</sub>)] in 1:1 molar ratio in acetone at 0 °C under an

Ar atmosphere. After 30 min of stirring, the acetone was completely removed, and the oily residues were treated with *n*-hexane, to give yellow solids that were filtered off and dried in air.

The most significant aspect of the spectroscopic data of these solids is the presence of a singlet signal with platinum satellites in the <sup>31</sup>P NMR spectrum, because this indicates that all of the solids correspond to complexes containing a Pt–PPh<sub>3</sub> bond. These spectroscopic data seem to indicate that, at least for complexes **1** and **3–5**, the PPh<sub>3</sub> ligand migrates from the silver center to the platinum center. In all cases, crystals suitable for X-ray diffraction analysis were obtained and identified as [Pt(bzq)(C<sub>6</sub>F<sub>5</sub>)(PPh<sub>3</sub>)<sub>2</sub>Ag]ClO<sub>4</sub> (**7**). In the case in which the starting material was [Pt(C<sub>6</sub>F<sub>5</sub>)(bzq)(PPh<sub>3</sub>)] (**2**), a second signal was also observed in the <sup>31</sup>P NMR spectrum of the resulting material. At room temperature, this signal is broad and resolves at –70 °C into a doublet of doublets, a pattern typical for a phosphorus atom bonded to a silver center (silver has two NMR active isotopes, <sup>107</sup>Ag, 51.8% abundance, and <sup>109</sup>Ag, 48.2% abundance). Crystals obtained from the crude solid could be also studied by X-ray diffraction, and they were identified as [Ag(PPh<sub>3</sub>)<sub>2</sub>](ClO<sub>4</sub>).

For the case in which the starting material was [Pt(C<sub>6</sub>F<sub>5</sub>)(bzq)(pyPh<sub>2</sub>)] (**3**), it was possible to obtain crystals that were identified through X-ray diffraction as the dinuclear [(C<sub>6</sub>F<sub>5</sub>)(bzq)(PPh<sub>3</sub>)PtAg(pyPh<sub>2</sub>)]ClO<sub>4</sub> (**11**) complex, which contains a donor–acceptor Pt→Ag bond (see below).

All these results are summarized in Scheme 3. It seems that migration of the PPh<sub>3</sub> ligand from Ag to Pt corresponds to a higher lability of the Pt–O bonds (when L = Me<sub>2</sub>CO), Pt–N bonds (when L = MeCN or pyPh<sub>2</sub>), or Pt–S bonds (when L = tbt) than the Pt–P bonds. The final formation of trinuclear sandwich **7** is probably caused by the final stability of this complex. The existence of [AgL<sub>2</sub>]<sup>+</sup> has only been confirmed for L = PPh<sub>3</sub>, but given the presence of signals in the IR and <sup>1</sup>H NMR spectra for other



Scheme 3.

diagnostic groups in L, it is sensible to assume an overall reaction process as depicted in Scheme 3 (b).

However, the identification of  $[(C_6F_5)(bzq)(PPh_3)PtAg(pyPh_2)]ClO_4$  (**11**) is interesting. Its existence could indicate that the formation of trinuclear **7** occurs through the pathway given in Scheme 3 (a). For some reason, intermediate compound **11** could only be detected in the case of L = pyPh<sub>2</sub>. Apart from evident electronic reasons, an important difference between the other L ligands used (i.e., Me<sub>2</sub>CO, MeCN, tht) and pyPh<sub>2</sub> is size and, thus, the resulting steric hindrance caused by the latter. Thus, kinetic effects could be the reason why **11** evolves more slowly than the rest of the complexes, and some crystals could be formed prior to its complete conversion into **7**.

### Crystal Structure of $[(C_6F_5)(bzq)(PPh_3)PtAg(pyPh_2)]ClO_4$ (**11**)

As mentioned above, the crystal structure of complex **11** was determined by X-ray diffraction. Figure 7 shows a view of the complex cation, and Table 7 lists a selection of relevant bond lengths and angles.

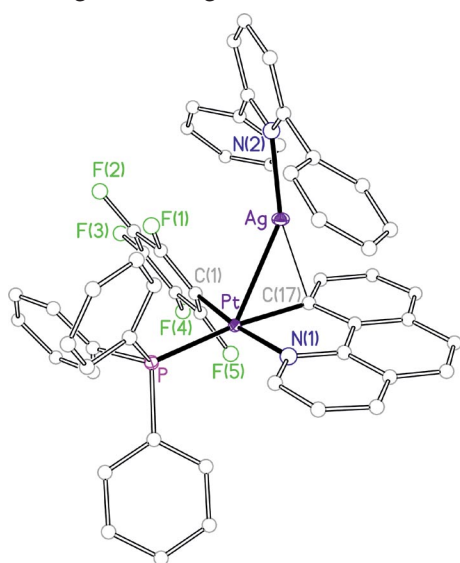


Figure 7. View of the molecular structure of the cation of  $[(C_6F_5)(bzq)(PPh_3)PtAg(pyPh_2)]ClO_4$  (**11**).

Table 7. Selected bond lengths and angles for  $[(Pt(C_6F_5)(bzq)(PPh_3))Ag(pyPh_2)]ClO_4 \cdot CH_2Cl_2$  (**11**·CH<sub>2</sub>Cl<sub>2</sub>).

Bond length [Å]			
Pt–C(1)	2.0140(13)	Pt–C(17)	2.0633(15)
Pt–N(1)	2.1143(11)	Pt–P	2.3286(4)
Pt–Ag	2.8147(1)	Ag–N(2)	2.1898(12)
Ag–C(17)	2.2929(14)		
Bond angle [°]			
C(1)–Pt–C(17)	92.64(6)	C(1)–Pt–N(1)	172.95(5)
C(17)–Pt–N(1)	80.42(5)	C(1)–Pt–P	89.90(4)
C(17)–Pt–P	173.14(4)	N(1)–Pt–P	97.13(4)
N(2)–Ag–Pt	146.48(3)		

This study confirms the presence of a donor–acceptor Pt→Ag bond in the structure, with an intermetallic dis-

tance of 2.8147(1) Å. This distance is similar to those found in  $\{[Pt(C_6F_5)(bzq)(PPh_3)]_2Ag\}ClO_4$  (**7**) [cf. 2.823(1) and 2.745(1) Å], which also contains the “Pt(C<sub>6</sub>F<sub>5</sub>)(bzq)(PPh<sub>3</sub>)” fragment. In contrast, it is slightly longer than those found in the analogous complexes  $[(C_6X_5)_2(bzq)PtAg(PPh_3)]^-$  [2.728(1) Å for X = F and 2.675(3) Å for X = Cl],<sup>[17]</sup> perhaps because of the anionic nature of these latter compounds in comparison with the neutral nature of **11**. Moreover, as described above for complexes **7**, **9**, and **10** and other similar “(bzq)Pt→Ag” complexes,<sup>[17,39]</sup> the silver center establishes an η<sup>1</sup>-Ag–C interaction with the *ipso* carbon atom of the bzq ligand with a Ag–C(17) distance of 2.293(1) Å. This value is shorter than the one found in **7** [cf. 2.351(4) and 2.460(3) Å], **9** [cf. 2.347(8) and 2.339(8) Å], and **10** [cf. 2.425(8) and 2.467(8) Å] and in  $[(C_6X_5)_2(bzq)PtAg(PPh_3)]^-$  [2.352(3) Å for X = F and 2.557(5) Å for X = Cl],<sup>[17]</sup> which seems to indicate a stronger interaction. In fact, the silver center clearly leans toward the C<sub>*ipso*</sub> position of the bzq ligand; the angle between the Pt–Ag line and the perpendicular of the best Pt square-plane is 44.6(1)°, which is a large value {compare with the analogous angles 32.1(1) and 24.7(1)° in **7**, 30.1(1) and 34.1(1)° in **9**, 32.4(2) and 32.6(2)° in **10**, 34.9(1)° in  $[(C_6F_5)_2(bzq)PtAg(PPh_3)]^-$ ,<sup>[17]</sup> and 27.2(1)° in  $[(C_6Cl_5)_2(bzq)PtAg(PPh_3)]^-$ ,<sup>[17]</sup>}, and the Pt–Ag–N(2) angle is 146.5(1)°. This “so bent” disposition is probably caused by the steric hindrance resulting from the two PPh<sub>3</sub> and pyPh<sub>2</sub> bulky ligands present in **11**, which try to stay as far away from one another as much as possible. The coordination sphere of the silver center is completed by the pyPh<sub>2</sub> ligand, with a Ag–N(2) distance of 2.190(1) Å, which is in the usual range for this type of bond.<sup>[90–95]</sup>

In this case, complex **11** does not show extended intermolecular interactions through π⋯π interactions of the planar aromatic rings of the bzq ligand.

## Photophysical Properties

### Absorption Spectra and Theoretical Calculations

The UV/Vis spectra data of compounds **1–11** in solution are summarized in Table S1 (Supporting Information). Data of precursor complex **1** are also included for comparison. In CH<sub>2</sub>Cl<sub>2</sub> solution (10<sup>−4</sup> M), mononuclear complexes **1–5** exhibit high-energy bands (range 250–380 nm), whose intensities and shapes are typical of <sup>1</sup>IL transitions (C<sub>6</sub>F<sub>5</sub>, bzq) that are somewhat perturbed by the coordination of platinum (see Figure 8 for complex **2**).<sup>[39,96,97]</sup> In addition, they show a modest shoulder ( $\epsilon = 1.0\text{--}2.1 \times 10^3 \text{ M}^{-1} \text{ cm}^{-1}$ ) centered at ca. 400 nm, which can generally be attributed to <sup>1</sup>MLCT/<sup>1</sup>IL transitions. The UV/Vis spectra of complexes **1–5** recorded in different solvents show modest solvatochromism (see Figure S3 in the Supporting Information for complex **2**) of the absorption bands, particularly in the lower-energy spectral region, which is characteristic of CT transitions.

The absorption spectra of heteronuclear complexes **6–11** are all quite similar to those of their respective precursors **1–5** as much in the solid state as in solution (Tables 8 and

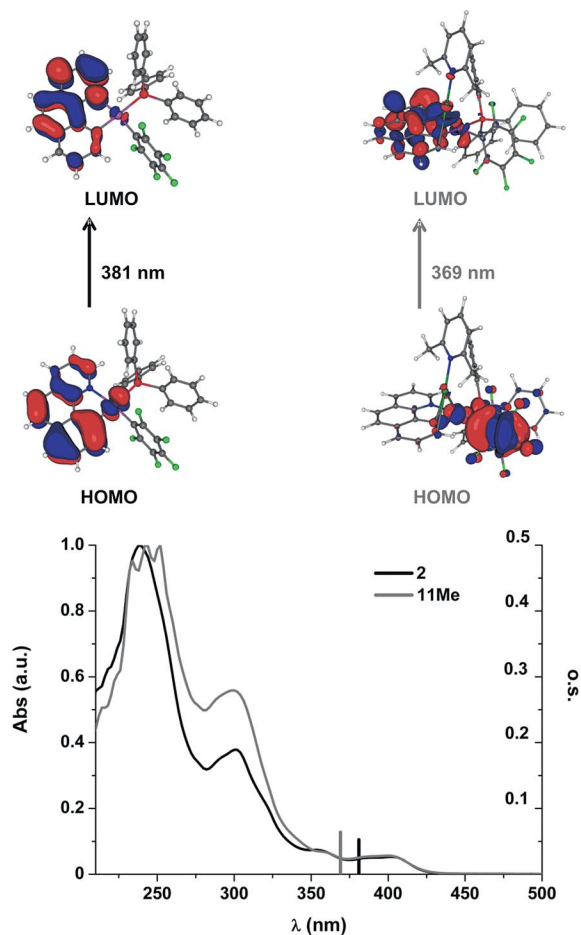


Figure 8. Frontier orbital plots for complexes **2** and **11Me** in  $\text{CH}_2\text{Cl}_2$  obtained by DFT calculations; calculated electronic transitions (bars) and experimental UV/Vis spectrum of **2** and **11** in  $\text{CH}_2\text{Cl}_2$  ( $10^{-4}$  M).

9, Figure 8; see also Table S1 and Figures S4 and S5 in the Supporting Information). Complexes containing Pt–Ag

datave bonds often show a blueshift in the low-energy absorption maxima; donation of electron density increases electrophilicity of the Pt center, which lowers the energy of the HOMO and raises the energy of the  $^1\text{MLCT}$  absorption bands.<sup>[17,39]</sup> In complexes **6–11**, little if any shift in the low-energy absorption maxima with respect to those of the starting compounds is observed. Similar behavior was previously observed in  $\text{CH}_2\text{Cl}_2$  solution of the trinuclear complex  $(\text{NBu}_4)[\{\text{Pt}(\text{bzq})(\text{C}_6\text{F}_5)_2\}_2\text{Ag}]$ ,<sup>[17]</sup> which was explained by the partial cleavage of the Pt–Ag bond in solution. However, this feature cannot be invoked in the solid state.

To better explain the nature of the lower-energy transitions, TD-DFT calculations were carried out by using the B3LYP hybrid density functional for **2**, **4**, and **5** and the M06 hybrid density functional for **9**, **10**, and **11Me** (**11Me** is a model complex derived from complex **11** by replacing the Ph groups with Me groups in the  $\text{pyPh}_2$  ligand to simplify the calculation process). The geometric parameters of the optimized  $\text{S}_0$  structures (Tables S2–S7, Supporting Information) agree well with the experimental values. Relevant data on the calculated lower-energy electronic transitions in  $\text{CH}_2\text{Cl}_2$  and the frontier molecular orbitals (MOs) involved in them are listed in Tables 10 and 11. In the mononuclear complexes, the HOMO is mostly constructed from orbitals located on the bzq ligand (75% in **5** to 84% in **2**) and the platinum center (23% in **5** to 14% in **2**). The LUMO is well located on the imine ring (ca. 95%). Figure 8 shows that the calculated lowest-energy electronic transition in  $\text{CH}_2\text{Cl}_2$  (bars) for compound **2** fits well, within the accuracy of the method, to the experimental absorptions. Calculations indicate that the major contribution to the lowest-lying absorption involves the HOMO→LUMO (94%) transition, which is indicative of a remarkable ligand-centered [ $^1\text{IL}$ ,  $\pi$ – $\pi^*$  (bzq)] mixed with some metal-to-ligand charge transfer [ $^1\text{MLCT}$   $5d(\text{Pt})\rightarrow\pi^*(\text{bzq})$ ] character. Contrary to other benzoquinolate  $\text{Pt}^{\text{II}}$  complexes described,<sup>[39,96,97]</sup> no ligand-to-ligand charge transfer

Table 8. Photophysical data for compounds **1–5** in the solid state.

Compound	$\lambda_{\text{absorption}}/\text{nm}$	$\lambda_{\text{exc}}/\text{nm}$	$\lambda_{\text{em}}/\text{nm}$	$\tau/\mu\text{s}$	
<b>1</b>	298 K	304, 394, 412 (tail to 450)	405	467, 482, 496, 578 <sub>max</sub>	[a]
	77 K		420	504, 540 <sub>max</sub> , 583	204 (44%), 21.0(56%), at 504 nm 212.2(40%), 25.6(60%), at 540 nm
<b>2</b>	298 K	301, 388, 405 (tail to 450)	390	481 <sub>max</sub> , 490, 515 <sub>max</sub> , 554, 599 <sub>sh</sub>	[a]
	77 K		390	479 <sub>max</sub> , 490, 515 <sub>max</sub> , 529 <sub>sh</sub> , 556, 596 <sub>sh</sub>	82.0(58%), 221.5(42%), at 479 nm, 42.1(28%), 107.0(72%), at 515 nm
<b>3</b>	298 K	302, 408, 427 (tail to 460)	410	497, 590 <sub>max</sub> , 632	[a]
	77 K		410	515, 529, 555 <sub>max</sub> , 590 <sub>sh</sub>	158.4(32%), 35.8 (68%), at 515 nm 242.7(25%), 40.7(75%), at 555 nm
<b>4</b>	298 K	303, 387, 402 (tail to 450)	400	594, 627 <sub>max</sub>	[a]
	77 K		400	512, 552 <sub>max</sub> , 596 <sub>sh</sub>	517.5(26%), 199.3 (74%), at 512 nm 440.1(42%), 147.0(58%), at 552 nm
<b>5</b>	298 K	307, 390, 405 (tail to 450)	390	482, 514, 580 <sub>sh</sub> , 632 <sub>max</sub>	[a]
	77 K		390	512, 549 <sub>max</sub>	366.8(39%), 90.7 (61%), at 512 nm 508.7(36%), 84.5(64%), at 549 nm

[a] Emission was too weak to be measured.

Table 9. Photophysical data for compounds **6–11** in the solid state.

Compound	$\lambda_{\text{absorption}}/\text{nm}$	$\lambda_{\text{exc}}/\text{nm}$	$\lambda_{\text{em}}/\text{nm} [\Phi]$	$\tau/\mu\text{s}$	
<b>6</b>	298 K	306, 335, 411 (tail to 550)	415	515 <sub>sh</sub> , 581 <sub>max</sub>	8.2(98%), 120.2 (2%), at 515 nm 6.7 (92%), 67.0 (8%), at 581 nm
	77 K		415	509, 597 <sub>max</sub>	18.7 at 509 nm, 16.9 at 597 nm
<b>7</b>	298 K	305, 324, 401 (tail to 460)	400	468 <sub>sh</sub> , 503, 530 <sub>max</sub> , 565 <sub>sh</sub> [0.032]	23.8 (86%), 79.1 (14%) at 502 nm 20.1 (40%), 78.2 (60%) at 528 nm
	77 K		400	492, 591 <sub>max</sub>	15.6 at 492 nm 21.7 (65%), 45.5 (35%), at 591 nm
<b>8</b>	298 K	303,342, 409 (tail to 485)	410	540 <sub>sh</sub> , 584 <sub>max</sub> , 630 <sub>sh</sub>	8.7 at 540 nm 3.1 (86%), 11.8(14%) at 584 nm
	77 K		410	500, 638 <sub>max</sub>	12.7 at 500 nm, 14.6 at 638 nm
<b>9</b>	298 K	300, 401 (tail to 460)	400	520 <sub>sh</sub> , 551 <sub>max</sub> , 575 <sub>sh</sub>	8.1 at 520 nm, 6.8 at 551 nm, 8.9 at 575 nm
	77 K		400	499, 607 <sub>max</sub>	19.4 at 499 nm, 33.2 at 607 nm
<b>10</b>	298 K	300, 336, 394, 408 (tail to 465)	390	514, 562 <sub>max</sub>	1.5 at 514 nm, 1.9 at 562 nm
	77 K		390	500, 540 <sub>sh</sub> , 601 <sub>max</sub>	14.2 at 500 nm, 19.5 at 540 nm, 15.8 at 601 nm
<b>11</b>	298 K	302, 397 (tail to 500)	370	490, 519 <sub>max</sub> , 554 [0.15]	17.6 at 490 nm, 17.9 at 519 nm, 18.0 at 554 nm
	77 K		370	480, 492 <sub>sh</sub> , 509 <sub>sh</sub> , 565 <sub>max</sub>	21.0 at 480 nm, 21.8 at 492 nm, 27.5 at 509 nm, 26.8 at 565 nm

Table 10. Population analysis [%] of frontier MOs in the ground state for [Pt(C<sub>6</sub>F<sub>5</sub>)(bzq)L] [L = PPh<sub>3</sub> (**2**), tht (**4**), MeCN (**5**)], [(C<sub>6</sub>F<sub>5</sub>)(bzq)(PPh<sub>3</sub>)PtAg(pyMe<sub>2</sub>)<sup>+</sup> (**11Me**), and [Pt(C<sub>6</sub>F<sub>5</sub>)(bzq)L<sub>2</sub>Ag]<sup>+</sup> [L = tht (**9**) and MeCN (**10**)].

	HOMO						LUMO					
	eV	Pt (1/2)	Ag	bzq	C <sub>6</sub> F <sub>5</sub>	L	eV	Pt (1/2)	Ag	bzq	C <sub>6</sub> F <sub>5</sub>	L
<b>2</b>	-5.68	14		84	0	2	-1.84	4		95	0	1
<b>11Me</b>	-8.71	12	0	4	77	6	-4.47	3	9	84	1	3
<b>4</b>	-5.71	20		79	0	1	-1.88	4		96	0	0
<b>9</b>	-8.64	16/16	10	55	2	1	-4.71	1/2	12	83	1	1
<b>5</b>	-5.59	23		75	0	2	-1.86	4		95	0	1
<b>10</b>	-8.58	22/2	6	56	13	1	-4.46	2/4	17	73	2	2

[<sup>1</sup>L/LCT, Ar<sub>r</sub>→bzq or L→bzq] transitions are involved in this absorption. In view of the data given in Tables 10 and 11 and Figures S4 and S5 (Supporting Information), the same assignments can be made for the lowest-lying absorption of compounds **4** and **5**, but in these cases, the transition shows slightly higher <sup>1</sup>MLCT character. The blueshift observed in the calculated lowest-energy transition of **2** (381 nm) in relation to that of the other mononuclear complexes (382 nm for **4** and 386 nm for **5**) can be due to the lower energy level of the dπ(Pt) orbitals because of the electron-withdrawing character of the PPh<sub>3</sub> ligand with respect to those of the tht and MeCN ligands,<sup>[98–101]</sup> as no significant contribution of the L ligands to the frontier orbitals was observed.

Table 11. Selected singlet excited states calculated by TD-DFT for complexes **2**, **4**, **5**, **9**, **10**, and **11Me** in CH<sub>2</sub>Cl<sub>2</sub> solution; o.s. = oscillator strength.

	$\lambda_{\text{exc}}$ (calcd.) [nm]	o.s.	Transition (% contribution)
<b>2</b>	381.2	0.0524	HOMO→LUMO (94.4)
<b>11Me</b>	369.3	0.0695	HOMO→LUMO (94.5)
<b>4</b>	382.2	0.0610	HOMO→LUMO (94.0)
<b>9</b>	405.2	0.0516	HOMO→LUMO (94.5)
<b>5</b>	386.9	0.0577	HOMO→LUMO (94.8)
<b>10</b>	385.3	0.0342	HOMO→LUMO (85.8)

Calculations performed on trinuclear complexes **9** and **10** show that the HOMO is constructed from orbitals located on the bzq ligand (ca. 55%) and the platinum centers (32% for **9**, 24% for **10**) and with less weight from silver (10% for **9**, 6% for **10**) and C<sub>6</sub>F<sub>5</sub> orbitals (2% for **9**, 13% for **10**). The LUMO is well located on the imine ring (83% for **9**, 73% for **10**) and the silver atom (12% for **9**, 17% for **10**). Therefore, it seems that the formation of two Pt–Ag bonds decreases the contribution from the bzq ligand and increases the metallic character (Pt/Ag) of the HOMO and LUMO orbitals with respect to those of the starting complexes.

In dinuclear complex **11Me**, the HOMO is mainly constructed from orbitals located on C<sub>6</sub>F<sub>5</sub> (77%) and the platinum center (12%) with no contribution from the atomic orbitals of the silver atom and only a marginal contribution from the bzq orbitals (4%). The LUMO is well located on the imine ring (84%) with only a small metallic character (3% Pt, 9% Ag). Therefore, the formation of a Pt–Ag bond in **11Me** changes dramatically the composition of the frontier orbitals, especially that of the HOMO, by decreasing the weight of the bzq orbitals and increasing those of the electron-withdrawing C<sub>6</sub>F<sub>5</sub> group, as it was observed previously for the dinuclear [Pt(bzq)(C<sub>6</sub>F<sub>5</sub>)<sub>2</sub>]AgL] (L = PPh<sub>3</sub>, tht) complexes.<sup>[39]</sup> Taking into account that the lowest-en-

ergy electronic absorption of each one of these heteronuclear complexes is associated with a HOMO  $\rightarrow$  LUMO transition (Table 11), it could be ascribed to  ${}^1\text{ILCT}/{}^1\text{MM}'\text{LCT} [\pi-\pi^*(\text{bzq})/\{d/s(\text{Pt},\text{Ag})\} \rightarrow \pi^*(\text{bzq})]$  for **9** and **10** and to mixed  ${}^1\text{MLCT}/{}^1\text{L}'\text{LCT} [\text{MLCT } 5d(\text{Pt}) \rightarrow \pi^*(\text{bzq})]/[\text{L}'\text{LCT}, \text{Ar}_r \rightarrow \text{bzq}]$  for **11Me**. Therefore, the formation of Pt–Ag bonds leads to the stabilization of the HOMO and LUMO orbitals and to a change in the nature of the electronic transitions; however, this has little effect on the energy of the transitions, and the transitions are not always shifted to higher energies.

The diffuse reflectance UV/Vis spectra of complexes **1–11** in the solid state exhibit similar profiles to those in solution (see Figure S6 in the Supporting Information for **1–5**). Therefore, the same origin of the absorptions can be presumed. This indicates that the  $\pi \cdots \pi$  interactions observed in the solid state (see parts b in Figures 2 and 4, see also Figures S1 and S2 in the Supporting Information) have a very small effect, if any, in the lowest-energy absorption maxima except for complex **3**, for which this absorption appears redshifted relative to that of the other mononuclear complexes.

### Emission Spectra

Complexes **1–5** are scarcely emissive in the solid state at room temperature but become brightly emissive at 77 K; they exhibit an asymmetric yellow emission whose excitation spectrum resembles the absorption one (see Table 8 and Figure 9 for complex **4**). Emission lifetimes are rather long and always fit to two components, as observed in many benzoquinolate Pt<sup>II</sup> complexes.<sup>[97]</sup> Therefore, the phosphorescent emission can be ascribed to an admixture of  ${}^3\text{IL}/{}^3\text{MLCT}$  excited states, probably with remarkable  ${}^3\text{IL}$  character, especially for complex **2**.

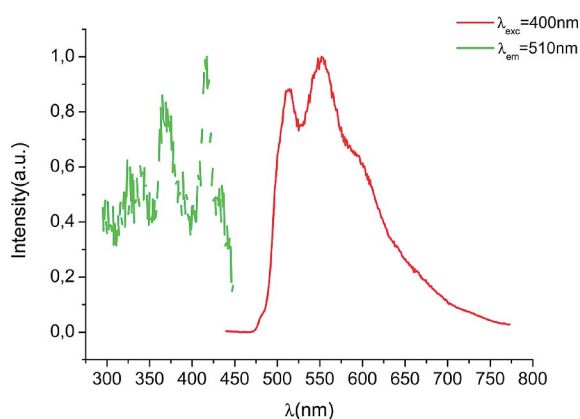


Figure 9. Normalized excitation and emission spectra of **4** in the solid state at 77 K.

Notably, at 298 K only compound **2** is moderately emissive (Figure 10, top). The emission (and excitation) profile of **2** is similar to that observed at 77 K and arises mainly from excited states originating in the monomer species. However, in compounds **1** and **3–5**, the weak emission seems to come from barely emissive aggregates.<sup>[18,102]</sup> By contrast, heteronuclear compounds **6–11** are emissive in the

solid state at room temperature (Figure 10, bottom), which shows that, in general, the presence of Pt–Ag dative bonds in heteronuclear compounds dramatically enhances the emission intensity when compared to that of their Pt<sup>II</sup> starting complexes.

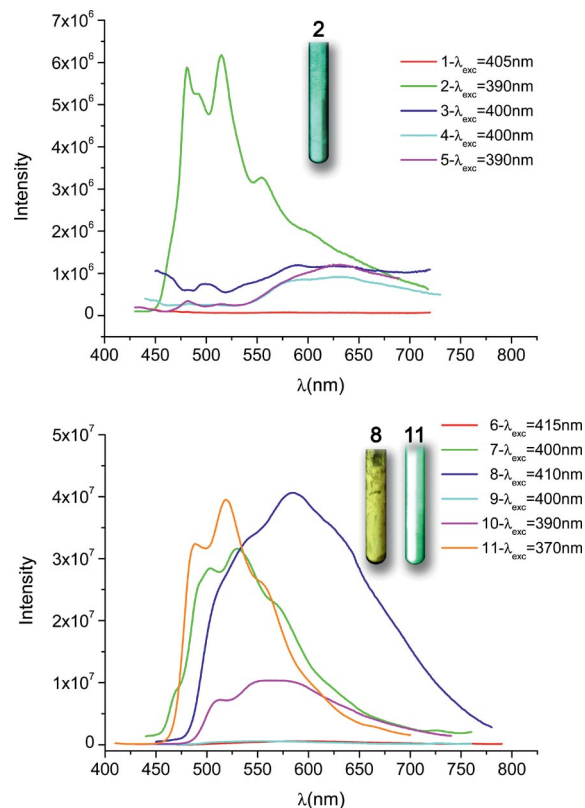


Figure 10. Top: Unnormalized emission spectra of **1–5** in the solid state at 298 K. Bottom: Unnormalized emission spectra of **6–11** in the solid state at 298 K; insets: compounds **2**, **8**, and **11** at 298 K upon excitation at  $\lambda = 365$  nm.

At 298 K, heteronuclear compounds **6–11** (Table 9 and Figure 10, bottom) exhibit a yellow-green ( $\lambda_{\text{max}} = 530$  nm for **7**,  $\lambda_{\text{max}} = 519$  nm **11**), yellow ( $\lambda_{\text{max}} = 551$  nm for **9**,  $\lambda_{\text{max}} = 562$  nm for **10**), and yellow-orange ( $\lambda_{\text{max}} = 581$  nm for **6**,  $\lambda_{\text{max}} = 584$  nm for **8**) phosphorescence, which is clearly enhanced upon cooling to 77 K.

Compounds **7** and **11**, which contain the “Pt(bzq)(C<sub>6</sub>F<sub>5</sub>)(PPh<sub>3</sub>)” fragment, have very similar emission spectra at 298 K (Figure 10, bottom) and also at 77 K (Figure 11). Taking into account the TD-DFT calculations performed for compound **11Me** and the emission behavior described previously for  $[\{\text{Pt}(\text{bzq})(\text{C}_6\text{F}_5)_2\}\text{Ag}(\text{PPh}_3)]$ ,<sup>[39]</sup> the emission band observed at 298 K can mainly arise from a mixed  ${}^3\text{MLCT}/{}^3\text{L}'\text{LCT}$  excited state. At 77 K, the emission clearly resolves into two bands: a weaker high-energy (HE) emission at ca. 490 nm and an intense, broad, asymmetrical low-energy (LE) band ( $\lambda_{\text{max}} = 591$  nm for **7**,  $\lambda_{\text{max}} = 565$  nm for **11**) with its maximum clearly redshifted with respect to that at 298 K. The HE emission, which resembles the emission of the corresponding precursor, can be tentatively assigned to the  ${}^3\text{IL}/{}^3\text{MLCT}$  excited state.

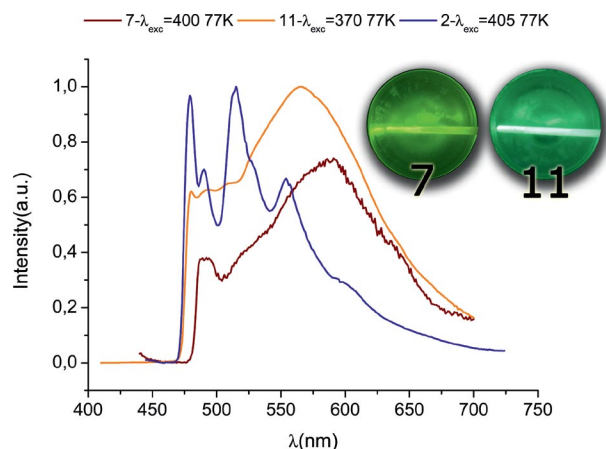


Figure 11. Normalized emission spectra of **2**, **7**, and **11** in the solid state at 77 K. Inset: Images of compounds **7** and **11** at 77 K upon excitation at  $\lambda = 365$  nm.

The emission spectra of trinuclear compounds **6** and **8–10** at 77 K show a profile that is similar to that of compound **7**, but their maxima are shifted to lower energies ( $\lambda_{\text{max}} = 597$  nm for **6**,  $\lambda_{\text{max}} = 638$  nm for **8**,  $\lambda_{\text{max}} = 607$  nm for **9**,  $\lambda_{\text{max}} = 601$  nm for **10**; see Figure S7 in the Supporting Information for complex **10**). TD-DFT calculations performed on complexes **9** and **10** show an important contribution from the metallic orbitals (Pt/Ag) to the frontier orbitals along with a small contribution from the  $\text{C}_6\text{F}_5$  orbitals. Because of this, it seems plausible to assign the more intense LE band observed in the spectra of **8–10** to a  ${}^3\text{MM}'\text{LCT}/{}^3\text{ILCT}$  emissive state.

Complexes **1–11** are emissive in a rigid matrix of  $\text{CH}_2\text{Cl}_2$  ( $10^{-3}$  M) at 77 K (Table S8, Supporting Information). Compounds **1–5** show several emissions upon excitation in the range 350–400 nm. They show low-intensity bands between 460 and 525 nm and a high-intensity asymmetric band centered at ca. 600 nm with a tail to 700 nm. 2-Methyltetrahydrofuran glassy solutions of **1–5** show similar profiles. At low concentration ( $10^{-5}$  M), the low-energy band shows similar energy and lifetime but a different profile to that in the solid state at 77 K (see Figures 9 and 12 for complex **4**),

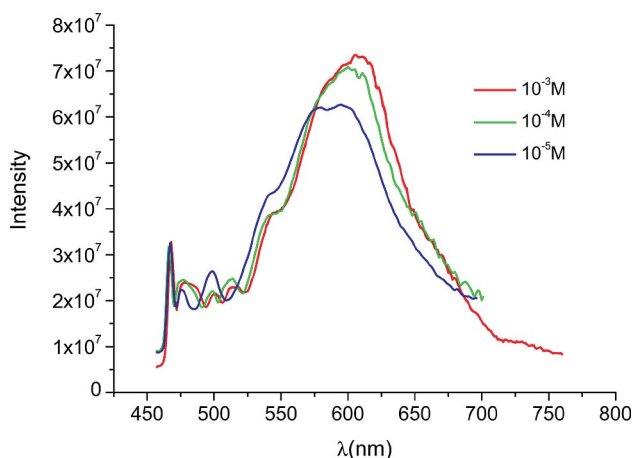


Figure 12. Emission spectra of **4** in  $\text{CH}_2\text{Cl}_2$  (77 K) at  $\lambda_{\text{exc}} = 400$  nm.

which could be attributed to a bigger deformation of the excited-state geometry in  $\text{CH}_2\text{Cl}_2$  at 77 K. The increasing intensity of the low-energy band with respect to the higher-energy bands with increasing concentration (from  $10^{-5}$  M to  $10^{-3}$  M) added to the redshift in its maximum (see Figure 12 for compound **4**), which suggests that emissive ground-state aggregates resulting from close  $\pi\cdots\pi$  intermolecular contacts could be not completely excluded at higher concentrations. The emission spectra of the heteronuclear compounds in a rigid matrix of  $\text{CH}_2\text{Cl}_2$  ( $10^{-3}$  M, 77 K, for **7–9** and **11**) showed similar profiles to those in the solid state at 77 K; therefore, the same origin can be presumed for these bands.

## Conclusions

Despite its neutral character,  $[\text{Pt}(\text{C}_6\text{F}_5)(\text{bzq})\text{L}]$  ( $\text{L} = \text{Me}_2\text{CO}$ ,  $\text{PPh}_3$ ,  $\text{pyPh}_2$ ,  $\text{tht}$ ,  $\text{MeCN}$ ) complexes have proven to be suitable precursors for the preparation of complexes containing Pt–Ag dative bonds. The bzq ligand seems to play an important role in the stabilization of the heteropolynuclear complexes formed in a twofold way. First, being a strong-field ligand, bzq raises the energy of the  $d_{z^2}$  platinum orbital and favors the formation of stronger  $\text{Pt} \rightarrow \text{Ag}$  dative bonds. Second, in these complexes the silver centers establish short  $\eta^1$  interactions with the  $\text{C}_{\text{ipso}}$  atom of the bzq ligand, which contribute to fulfil the electron density requirements of the acidic silver center. Nevertheless, only trimetallic “sandwich”  $[\{\text{Pt}(\text{C}_6\text{F}_5)(\text{bzq})\text{L}\}_2\text{Ag}]^+$  complexes can be prepared, even if other Pt/Ag ratios are used. Therefore, it seems that the silver center “needs” to be surrounded by two  $[\text{Pt}(\text{C}_6\text{F}_5)(\text{bzq})\text{L}]$  subunits, with their corresponding Pt–Ag and Ag– $\text{C}_{\text{ipso}}$  interactions. This is in contrast to the  $[\{\text{Pt}(\text{bzq})(\text{C}_6\text{F}_5)_2\}\text{Ag}(\text{L})]$  and  $[\{\text{Pt}(\text{bzq})(\text{C}_6\text{F}_5)_2\}\text{Ag}]_x$  complexes, for which the Pt/Ag ratio is 1:1, obtained from the  $[\text{Pt}(\text{bzq})(\text{C}_6\text{F}_5)_2]^-$  anion, in which, in principle, the Pt center has an excess amount of electron density. Only in one case was the 1:1  $[(\text{C}_6\text{F}_5)(\text{bzq})(\text{PPh}_3)\text{PtAg}(\text{pyPh}_2)]\text{ClO}_4$  (**11**) product observed, and its relative stability was caused by the presence of bulkier ligands that slow down its transformation into  $[\{\text{Pt}(\text{C}_6\text{F}_5)(\text{bzq})(\text{PPh}_3)\}_2\text{Ag}]\text{ClO}_4$  (**7**).

Moreover,  $[\{\text{Pt}(\text{C}_6\text{F}_5)(\text{bzq})\text{L}\}_2\text{Ag}]^+$  complexes are flexible and are able to adapt their geometry (to some extent) to the bulkiness of the ancillary L ligands to preserve, at the same time, the Pt–Ag and Ag– $\text{C}_{\text{ipso}}$  interactions.

The photophysical properties of these complexes were discussed with the aid of TD-DFT calculations on several compounds (i.e., **2**, **4**, **5**, **9**, **10**, and **11**Me in  $\text{CH}_2\text{Cl}_2$ ). In the mononuclear complexes the lower-lying absorption bands are ascribed to mixed  ${}^1\text{IL}$ ,  $\pi\text{--}\pi^*(\text{bzq})/[{}^1\text{MLCT } 5d(\text{Pt}) \rightarrow \pi^*(\text{bzq})]$  transitions, whereas in the heteronuclear compounds, the formation of Pt–Ag bonds changes the character of the transition to  ${}^1\text{ILCT}/{}^1\text{MM}'\text{LCT}$   $[\pi\text{--}\pi^*(\text{bzq})/\{d/s(\text{Pt}, \text{Ag})\} \rightarrow \pi^*(\text{bzq})]$  for the trinuclear complexes and to mixed  ${}^1\text{MLCT}/{}^1\text{L}'\text{LCT}$   $[\text{MLCT } 5d(\text{Pt}) \rightarrow \pi^*(\text{bzq})/[{}^1\text{L}'\text{LCT}, \text{Ar}_i \rightarrow \text{bzq}]$  for dinuclear complex **11**. However, although the formation of the Pt–Ag bonds perturbs the frontier orbitals, it does not always shift

the HOMO → LUMO transition to higher energies. With the exception of compound **2**, the mononuclear complexes are not emissive in the solid state at room temperature. However the heteronuclear compounds are. All compounds become brightly emissive in the solid state at 77 K. For all compounds, the main phosphorescent emission has been tentatively associated with a transition similar in character to their lowest-lying absorption.

## Experimental Section

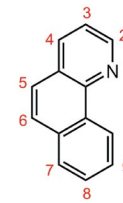
**Physical Measurements:** C, H, and N analyses, conductivity, and IR and NMR spectra were performed as described elsewhere.<sup>[16]</sup> <sup>1</sup>H, <sup>19</sup>F, and <sup>31</sup>P NMR spectra were recorded at 400, 376.5, and 162.0 MHz, respectively. Diffuse reflectance UV/Vis (DRUV) spectra were recorded with a Thermo electron corporation evolution 600 spectrophotometer equipped with a Praying Mantis integrating sphere. The solid samples were homogeneously diluted with silica. The mixtures were placed in a homemade cell equipped with quartz window. Steady-state photoluminescence spectra were recorded with a Jobin–Yvon Horiba Fluorolog FL-3–11 Tau 3 spectrofluorometer by using a slit width of 3 nm for both excitation and emission. Phosphorescence lifetimes were recorded with a Fluoromax phosphorimeter accessory containing a UV xenon flash tube with a flash rate between 0.05 and 25 Hz. Phase shift and modulation were recorded over the frequency range of 0.1–100 MHz. Nanosecond lifetimes were recorded with an IBH 5000F Coaxial nanosecond flashlamp. The lifetime data were fitted by using the Jobin–Yvon software package and the Origin Pro 8 program. The quantum efficiency was determined by using Quantaurus quantum yield equipment from Hamamatsu model C11347-11.

**Preparations:** Literature methods were used to prepare the [Pt(C<sub>6</sub>F<sub>5</sub>)(bzq)(Me<sub>2</sub>CO)] (**1**) starting material.<sup>[60]</sup>

**Caution!** Perchlorate salts of metal complexes with organic ligands are potentially explosive. Only small amounts of material should be prepared and these should be handled with great care.

**Preparation of [Pt(C<sub>6</sub>F<sub>5</sub>)(bzq)L] [L = PPh<sub>3</sub> (**2**), pyPh<sub>2</sub> (**3**), tht (**4**):** To a solution of [Pt(bzq)(C<sub>6</sub>F<sub>5</sub>)(Me<sub>2</sub>CO)] (**1**; 0.200 g, 0.335 mmol) in Me<sub>2</sub>CO (10 mL) at 0 °C and under an Ar atmosphere was added L (0.335 mmol; L = PPh<sub>3</sub>, 0.0879 g; pyPh<sub>2</sub>, 0.0775 g; tht, 30 μL). After 2 min of stirring, the solution was concentrated to ca. 2 mL. The yellow precipitate that appeared was filtered off, washed with *n*-hexane (10 mL), and air dried.

**[Pt(C<sub>6</sub>F<sub>5</sub>)(bzq)(PPh<sub>3</sub>) (**2**):** Yield 0.242 g, 90%. C<sub>37</sub>H<sub>22</sub>F<sub>5</sub>NPpt (801.63): calcd. C 55.37, H 2.89, N 1.75; found C 55.32, H 2.90, N 1.79. IR:  $\tilde{\nu}$  = 1498 (w), 1458 (w), 1433 (w), 1096 (w,  $\nu_{\text{PPh}_3}$ ), 1058 (w), 955 (m), 804 (m, C<sub>6</sub>F<sub>5</sub>, X-sensitive vibr.),<sup>[103]</sup> 693 (w), 529 (m), 509 (m) cm<sup>-1</sup>.  $A_M$  (Me<sub>2</sub>CO) = 4.17 Ω<sup>-1</sup> cm<sup>2</sup> mol<sup>-1</sup>. <sup>1</sup>H NMR ([D<sub>6</sub>]Me<sub>2</sub>CO, 295 K):  $\delta$  = 8.55 (dd, <sup>3</sup>J<sub>H<sub>4</sub>H<sub>3</sub></sub> = 8.08 Hz, <sup>4</sup>J<sub>H<sub>4</sub>H<sub>2</sub></sub> = 1.25 Hz, H<sub>4</sub>), 8.33 (dd, <sup>3</sup>J<sub>H<sub>2</sub>H<sub>3</sub></sub> = 5.35 Hz, <sup>4</sup>J<sub>H<sub>2</sub>H<sub>4</sub></sub> = 1.07 Hz, <sup>3</sup>J<sub>Pt,H<sub>2</sub></sub> = 26.85 Hz, H<sub>2</sub>), 7.93 (d, <sup>3</sup>J<sub>H<sub>5</sub>H<sub>6</sub></sub> = 8.72 Hz, H<sub>5</sub>), 7.78 (m, overlapped with 6H-*m*-Ph and H<sub>7</sub>, H<sub>6</sub>), 7.78 (m, overlapped with 6H-*m*-Ph and H<sub>6</sub>, H<sub>7</sub>), 7.78 (m, overlapped with H<sub>6</sub> and H<sub>7</sub>, 6H-*m*-Ph), 7.51 (m,  $J_{\text{H}_{\text{para}},\text{H}_{\text{meta}}} = 7.50$  Hz,  $J_{\text{H}_{\text{para}},\text{H}_{\text{ortho}}} = 1.60$  Hz, 3H-*p*-Ph), 7.43 (m, overlapped with 6H-*o*-Ph, H<sub>8</sub>), 7.43 (m, overlapped with H<sub>8</sub>, 6H-*o*-Ph), 7.23 (dd, <sup>3</sup>J<sub>H<sub>3</sub>H<sub>4</sub></sub> = 8.06 Hz, <sup>3</sup>J<sub>H<sub>3</sub>H<sub>2</sub></sub> = 5.37 Hz, H<sub>3</sub>), 7.00 (dd, <sup>3</sup>J<sub>H<sub>9</sub>H<sub>8</sub></sub> = 7.26 Hz, <sup>3</sup>J<sub>H<sub>9</sub>H<sub>7</sub></sub> = 6.22 Hz, <sup>3</sup>J<sub>Pt,H<sub>9</sub></sub> = 52.01 Hz, H<sub>9</sub>) ppm. <sup>19</sup>F NMR ([D<sub>6</sub>]Me<sub>2</sub>CO, 295 K):  $\delta$  = -118.50 (<sup>3</sup>J<sub>F,Pt</sub> = 508.6 Hz, *o*-F), 167.94 (br. m, *m*-F), -168.37 (*p*-F) ppm. <sup>31</sup>P NMR ([D<sub>6</sub>]Me<sub>2</sub>CO, 295 K):  $\delta$  = 28.05 (s,  $J_{\text{P,Pt}} = 1982.2$  Hz) ppm.



**[Pt(C<sub>6</sub>F<sub>5</sub>)(bzq)(pyPh<sub>2</sub>) (**3**):** Yield 0.220 g, 85%. C<sub>36</sub>H<sub>21</sub>F<sub>5</sub>N<sub>2</sub>Pt (771.65): calcd. C 56.03, H 2.74, N 3.63; found C 55.88, H 2.86, N 3.52. IR:  $\tilde{\nu}$  = 1497 (w), 1448 (m), 1435 (w), 1056 (w), 951 (m), 793 (m, C<sub>6</sub>F<sub>5</sub>, X-sensitive vibr.),<sup>[103]</sup> 696 (m,  $\nu_{\text{pyPh}_2}$ ) cm<sup>-1</sup>.  $A_M$  (Me<sub>2</sub>CO) = 5.66 Ω<sup>-1</sup> cm<sup>2</sup> mol<sup>-1</sup>. <sup>1</sup>H NMR ([D<sub>6</sub>]Me<sub>2</sub>CO, 295 K):  $\delta$  = 8.67 (m, <sup>3</sup>J<sub>H<sub>2</sub>H<sub>3</sub></sub> = 5.30 Hz, H<sub>2</sub>), 8.64 (d, <sup>3</sup>J<sub>H<sub>4</sub>H<sub>3</sub></sub> = 8.10 Hz, <sup>4</sup>J<sub>H<sub>4</sub>H<sub>2</sub></sub> = 1.20 Hz, H<sub>4</sub>), 8.26 (m, <sup>3</sup>J<sub>H<sub>meta</sub>,H<sub>ortho</sub></sub> = 7.09 Hz, <sup>4</sup>J<sub>H<sub>para</sub>,H<sub>ortho</sub></sub> = 1.50 Hz, 4H-*o*-Ph), 7.98–7.86 (m, overlapped signals of 2H-*m*-py and H-*p*-py), 7.85 (d, <sup>3</sup>J<sub>H<sub>5</sub>H<sub>6</sub></sub> = 8.80 Hz, H<sub>5</sub>), 7.78 (d, <sup>3</sup>J<sub>H<sub>6</sub>H<sub>5</sub></sub> = 8.80 Hz, H<sub>6</sub>), 7.73 (m, overlapped with H<sub>2</sub> and H<sub>4</sub>, H<sub>3</sub>), 7.56 (d, <sup>3</sup>J<sub>H<sub>7</sub>H<sub>8</sub></sub> = 7.97 Hz, H<sub>7</sub>), 7.53 (m, <sup>3</sup>J<sub>H<sub>meta</sub>,H<sub>ortho</sub></sub> = 7.45 Hz, <sup>3</sup>J<sub>H<sub>para</sub>,H<sub>meta</sub></sub> = 1.40 Hz, 4H-*m*-Ph), 7.46 (tt, <sup>3</sup>J<sub>H<sub>para</sub>,H<sub>meta</sub></sub> = 7.28 Hz, <sup>4</sup>J<sub>H<sub>para</sub>,H<sub>ortho</sub></sub> = 1.30 Hz, 2H-*p*-Ph), 7.25 (dd, <sup>3</sup>J<sub>H<sub>8</sub>H<sub>7</sub></sub> = 7.66 Hz, <sup>3</sup>J<sub>H<sub>8</sub>H<sub>9</sub></sub> = 7.35 Hz, H<sub>8</sub>), 6.89 (dd, <sup>3</sup>J<sub>H<sub>9</sub>H<sub>8</sub></sub> = 7.35 Hz, <sup>3</sup>J<sub>H<sub>9</sub>Pt</sub> = 74.1 Hz, H<sub>9</sub>) ppm. <sup>19</sup>F NMR (CD<sub>2</sub>Cl<sub>2</sub>, 295 K):  $\delta$  = -119.04 (<sup>3</sup>J<sub>F,Pt</sub> = 513 Hz, *o*-F), -166.61 (*p*-F, t), 167.75 (*m*-F, br. m) ppm.

**[Pt(C<sub>6</sub>F<sub>5</sub>)(bzq)(tht) (**4**):** Yield 0.214 g, 98%. C<sub>23</sub>H<sub>16</sub>F<sub>5</sub>NPtS (628.52): calcd. C 43.95, H 2.57, N 2.23, S 5.10; found C 44.08, H 2.32, N 2.33, S 5.10. IR:  $\tilde{\nu}$  = 1501 (m), 1451 (m), 1437 (m), 1267 (w,  $\nu_{\text{SC}}$ ), 1255 (w,  $\nu_{\text{SC}}$ ), 1061 (m), 951 (s), 798 (m, C<sub>6</sub>F<sub>5</sub>, X-sensitive vibr.) cm<sup>-1</sup>.<sup>[103]</sup>  $A_M$  (Me<sub>2</sub>CO) = 0.2 Ω<sup>-1</sup> cm<sup>2</sup> mol<sup>-1</sup>. <sup>1</sup>H NMR ([D<sub>6</sub>]Me<sub>2</sub>CO, 295 K):  $\delta$  = 9.35 (dd, <sup>3</sup>J<sub>H<sub>2</sub>H<sub>3</sub></sub> = 5.24 Hz, <sup>4</sup>J<sub>H<sub>2</sub>H<sub>4</sub></sub> = 1.31 Hz, <sup>3</sup>J<sub>H<sub>2</sub>Pt</sub> = 23.4 Hz, H<sub>2</sub>), 8.70 (dd, <sup>3</sup>J<sub>H<sub>4</sub>H<sub>3</sub></sub> = 8.08 Hz, <sup>4</sup>J<sub>H<sub>4</sub>H<sub>2</sub></sub> = 1.26 Hz, H<sub>4</sub>), 7.89 (d, <sup>3</sup>J<sub>H<sub>5</sub>H<sub>6</sub></sub> = 8.76 Hz, H<sub>5</sub>), 7.84 (dd, <sup>3</sup>J<sub>H<sub>3</sub>H<sub>4</sub></sub> = 8.08 Hz, <sup>3</sup>J<sub>H<sub>3</sub>H<sub>2</sub></sub> = 5.26 Hz, H<sub>3</sub>), 7.80 (d, <sup>3</sup>J<sub>H<sub>6</sub>H<sub>5</sub></sub> = 8.75 Hz, H<sub>6</sub>), 7.63 (dd, <sup>3</sup>J<sub>H<sub>7</sub>H<sub>8</sub></sub> = 7.92 Hz, <sup>4</sup>J<sub>H<sub>7</sub>H<sub>9</sub></sub> = 0.70 Hz, H<sub>7</sub>), 7.34 (dd, <sup>3</sup>J<sub>H<sub>8</sub>H<sub>9</sub></sub> = 8.04 Hz, <sup>3</sup>J<sub>H<sub>8</sub>H<sub>7</sub></sub> = 7.31 Hz, H<sub>8</sub>), 6.82 (d, <sup>3</sup>J<sub>H<sub>9</sub>H<sub>8</sub></sub> = 6.76 Hz, <sup>3</sup>J<sub>H<sub>9</sub>Pt</sub> = 62.01 Hz, H<sub>9</sub>), 3.23 (m, 4H-*m*-tht), 1.87 (m, 4H-*o*-tht) ppm. <sup>19</sup>F NMR ([D<sub>6</sub>]Me<sub>2</sub>CO, 295 K):  $\delta$  = -118.82 (<sup>3</sup>J<sub>F,Pt</sub> = 512.53 Hz, *o*-F), -166.09 (*p*-F), -166.90 (*m*-F, br. m) ppm.

**Preparation of [Pt(C<sub>6</sub>F<sub>5</sub>)(bzq)(MeCN)] (**5**):** Complex [Pt(bzq)(C<sub>6</sub>F<sub>5</sub>)(Me<sub>2</sub>CO)] (**1**) (0.200 g, 0.335 mmol) was dissolved in MeCN (10 mL) at 0 °C under an Ar atmosphere. After 2 min of stirring, the solution was evaporated to dryness. The yellow residue was treated with *n*-hexane (10 mL), filtered, and finally air dried. Yield 0.179 g, 92%. C<sub>21</sub>H<sub>11</sub>F<sub>5</sub>N<sub>2</sub>Pt (581.40): calcd. C 43.38, H 1.91, N 4.82; found C 42.99, H 1.79, N 4.71. IR:  $\tilde{\nu}$  = 2154 (vw,  $\nu_{\text{CN}}$ ), 1497 (m), 1453 (m), 1062 (m), 953 (vs), 798 (m, C<sub>6</sub>F<sub>5</sub>, X-sensitive vibr.) cm<sup>-1</sup>.<sup>[103]</sup>  $A_M$  (Me<sub>2</sub>CO) = 7.01 Ω<sup>-1</sup> cm<sup>2</sup> mol<sup>-1</sup>. <sup>1</sup>H NMR ([D<sub>6</sub>]Me<sub>2</sub>CO, 295 K):  $\delta$  = 9.19 (dd, <sup>3</sup>J<sub>H<sub>2</sub>H<sub>3</sub></sub> = 5.18 Hz, <sup>4</sup>J<sub>H<sub>4</sub>H<sub>2</sub></sub> = 1.20 Hz, <sup>3</sup>J<sub>H<sub>2</sub>Pt</sub> = 21.78 Hz, H<sub>2</sub>), 8.65 (dd, <sup>3</sup>J<sub>H<sub>4</sub>H<sub>3</sub></sub> = 8.06 Hz, <sup>3</sup>J<sub>H<sub>4</sub>H<sub>2</sub></sub> = 1.20 Hz, H<sub>4</sub>), 7.85 (d, <sup>3</sup>J<sub>H<sub>5</sub>H<sub>6</sub></sub> = 8.83 Hz, H<sub>5</sub>), 7.75 (d, <sup>3</sup>J<sub>H<sub>6</sub>H<sub>5</sub></sub> = 8.83 Hz, H<sub>6</sub>), 7.74 (d, <sup>3</sup>J<sub>H<sub>3</sub>H<sub>4</sub></sub> = 8.46 Hz, <sup>3</sup>J<sub>H<sub>3</sub>H<sub>2</sub></sub> = 5.00 Hz, overlapped with H<sub>6</sub>, H<sub>3</sub>), 7.58 (dd, <sup>3</sup>J<sub>H<sub>7</sub>H<sub>8</sub></sub> = 7.88 Hz, <sup>4</sup>J<sub>H<sub>7</sub>H<sub>9</sub></sub> = 0.60 Hz, H<sub>7</sub>), 7.30 (dd, <sup>3</sup>J<sub>H<sub>7</sub>H<sub>8</sub></sub> = 7.82 Hz, <sup>3</sup>J<sub>H<sub>7</sub>H<sub>9</sub></sub> = 7.62 Hz, H<sub>8</sub>), 6.96 (d, <sup>3</sup>J<sub>H<sub>9</sub>H<sub>8</sub></sub> = 7.62 Hz, <sup>3</sup>J<sub>H<sub>9</sub>Pt</sub> = 58.51 Hz, H<sub>9</sub>), 2.61 (s, H<sub>MeCN</sub>) ppm. <sup>19</sup>F NMR ([D<sub>6</sub>]Me<sub>2</sub>CO, 295 K):  $\delta$  = -119.08 (<sup>3</sup>J<sub>F,Pt</sub> = 513 Hz, *o*-F), -167.12 (*p*-F), 168.05 (*m*-F, br. m) ppm.

**Preparation of [Pt(C<sub>6</sub>F<sub>5</sub>)(bzq)L<sub>2</sub>Ag]ClO<sub>4</sub> [L = Me<sub>2</sub>CO (**6**), PPh<sub>3</sub> (**7**), pyPh<sub>2</sub> (**8**), tht (**9**):** To a solution of [Pt(bzq)(C<sub>6</sub>F<sub>5</sub>)L] (L = Me<sub>2</sub>CO, 0.250 g, 0.418 mmol; L = PPh<sub>3</sub>, 0.250 g, 0.187 mmol; L = pyPh<sub>2</sub>, 0.200 g, 0.260 mmol; L = tht, 0.200 g, 0.385 mmol) in Me<sub>2</sub>CO (20 mL) at 0 °C and under an Ar atmosphere was added AgClO<sub>4</sub> (L = Me<sub>2</sub>CO, 0.043 g, 0.209 mmol; L = PPh<sub>3</sub>, 0.019 g,

0.093 mmol; L = pyPh<sub>2</sub>, 0.0270 g, 0.130 mmol, L = tht, 0.040 g, 0.193 mmol). After 30 min of stirring in the absence of light, the solution was concentrated to ca. 2 mL. Over the resultant yellow suspension, *n*-hexane (10 mL) was added. The yellow precipitate was filtered off and air dried.

**[Pt(C<sub>6</sub>F<sub>5</sub>)(bzq)(Me<sub>2</sub>CO)]<sub>2</sub>AgClO<sub>4</sub> (6):** Yield 0.154 g, 56%. C<sub>44</sub>H<sub>28</sub>AgClF<sub>10</sub>N<sub>2</sub>O<sub>6</sub>Pt<sub>2</sub> (1404.18): calcd. C 37.64, H 2.01, N 2.00; found C 37.87, H 2.11, N 1.99. IR:  $\tilde{\nu}$  = 1620 (w), 1503 (w), 1455 (w), 1442 (w), 1096 (m,  $\nu_{\text{ClO}_4^-}$ ), 1059 (m), 953 (m), 801 (m, C<sub>6</sub>F<sub>5</sub>, X-sensitive vibr.),<sup>[103]</sup> 621 (m,  $\nu_{\text{ClO}_4^-}$ ) cm<sup>-1</sup>.  $A_M$  (Me<sub>2</sub>CO) = 134.35  $\Omega^{-1}$  cm<sup>2</sup> mol<sup>-1</sup>. <sup>1</sup>H NMR ([D<sub>6</sub>]Me<sub>2</sub>CO, 295 K):  $\delta$  = 8.70 (dd, <sup>3</sup>J<sub>H<sub>2</sub>,H<sub>3</sub></sub> = 8.11 Hz, <sup>4</sup>J<sub>H<sub>2</sub>,H<sub>4</sub></sub> = 1.14 Hz, H2), 8.64 (m, <sup>3</sup>J<sub>H<sub>4</sub>,H<sub>3</sub></sub> = 8.11 Hz, H4), 7.86 (m, H3, H5, and H6), 7.63 (dd, <sup>3</sup>J<sub>H<sub>7</sub>,H<sub>8</sub></sub> = 7.94 Hz, <sup>4</sup>J<sub>H<sub>7</sub>,H<sub>9</sub></sub> = 0.52 Hz, H7), 7.19 (dd, <sup>3</sup>J<sub>H<sub>8</sub>,H<sub>7</sub></sub> = 7.47 Hz, <sup>3</sup>J<sub>H<sub>8</sub>,H<sub>9</sub></sub> = 7.58 Hz, H8), 6.90 (d, <sup>3</sup>J<sub>H<sub>9</sub>,H<sub>8</sub></sub> = 7.06 Hz, <sup>3</sup>J<sub>H<sub>9</sub>,Pt</sub> = 71.21 Hz, H9), 2.14 (s, H<sub>Me<sub>2</sub>CO</sub>) ppm. <sup>19</sup>F NMR ([D<sub>6</sub>]Me<sub>2</sub>CO, 295 K):  $\delta$  = -117.89 (<sup>3</sup>J<sub>F,Pt</sub> = 502.3 Hz, *o*-F), -165.06 (*p*-F), -166.66 (br. m, *m*-F) ppm.

**[Pt(C<sub>6</sub>F<sub>5</sub>)(bzq)(PPh<sub>3</sub>)<sub>2</sub>AgClO<sub>4</sub> (7):** Yield 0.132 g, 82%. C<sub>74</sub>H<sub>46</sub>AgClF<sub>10</sub>N<sub>2</sub>O<sub>4</sub>P<sub>2</sub>Pt<sub>2</sub> (1812.60): calcd. C 49.03, H 2.56, N 1.55; found C 48.98, H 2.59, N 1.59. IR:  $\tilde{\nu}$  = 1500 (m), 1458 (m), 1435 (m), 1093 (m,  $\nu_{\text{ClO}_4^-}$ ), 1060 (m), 954 (s), 804 (s, C<sub>6</sub>F<sub>5</sub>, X-sensitive vibr.),<sup>[103]</sup> 693 (s), 621 (m,  $\nu_{\text{ClO}_4^-}$ ), 529 (s,  $\nu_{\text{PPh}_3}$ ), 509 (s,  $\nu_{\text{PPh}_3}$ ) cm<sup>-1</sup>.  $A_M$  (Me<sub>2</sub>CO) = 266.06  $\Omega^{-1}$  cm<sup>2</sup> mol<sup>-1</sup>. <sup>1</sup>H NMR ([D<sub>6</sub>]Me<sub>2</sub>CO, 295 K):  $\delta$  = 8.61 (dd, <sup>3</sup>J<sub>H<sub>4</sub>,H<sub>3</sub></sub> = 8.05 Hz, <sup>4</sup>J<sub>H<sub>4</sub>,H<sub>2</sub></sub> = 0.90 Hz, H4), 8.34 (d, <sup>3</sup>J<sub>H<sub>2</sub>,H<sub>3</sub></sub> = 5.35 Hz, <sup>3</sup>J<sub>H<sub>2</sub>,Pt</sub> = 25.77 Hz, H2), 7.94 (d, <sup>3</sup>J<sub>H<sub>5</sub>,H<sub>6</sub></sub> = 8.72 Hz, H5), 7.82 (d, <sup>3</sup>J<sub>H<sub>6</sub>,H<sub>5</sub></sub> = 8.74 Hz, H6), 7.74 (m, overlapped with 6H-*m*-Ph, H7), 7.53 (m, <sup>3</sup>J<sub>H<sub>para</sub>,H<sub>meta</sub></sub> = 7.46 Hz, <sup>3</sup>J<sub>H<sub>ortho</sub></sub> = 1.18 Hz, 3H-*p*-Ph), 7.45 (m, H8 and 6H-*o*-Ph), 7.29 (dd, <sup>3</sup>J<sub>H<sub>3</sub>,H<sub>4</sub></sub> = 8.05 Hz, <sup>3</sup>J<sub>H<sub>3</sub>,H<sub>2</sub></sub> = 5.37 Hz, H3), 7.11 (t, <sup>3</sup>J<sub>H<sub>9</sub>,H<sub>8</sub></sub> = 6.22 Hz, <sup>3</sup>J<sub>H<sub>9</sub>,Pt</sub> = 49.30 Hz, H9) ppm. <sup>19</sup>F NMR ([D<sub>6</sub>]Me<sub>2</sub>CO, 295 K):  $\delta$  = -117.89 (<sup>3</sup>J<sub>F,Pt</sub> = 504.3 Hz, *o*-F), -167.07, -167.54 (*m*-F, *p*-F br. m) ppm. <sup>31</sup>P NMR ([D<sub>6</sub>]Me<sub>2</sub>CO, 295 K):  $\delta$  = 27.23 (s,  $J_{\text{P,Pt}}$  = 2081.1 Hz) ppm.

**[Pt(C<sub>6</sub>F<sub>5</sub>)(bzq)(pyPh<sub>2</sub>)<sub>2</sub>AgClO<sub>4</sub> (8):** Yield 0.207 g, 96%. C<sub>72</sub>H<sub>42</sub>AgClF<sub>10</sub>N<sub>4</sub>O<sub>4</sub>Pt<sub>2</sub> (1750.61): calcd. C 49.40, H 2.42, N 3.20; found C 48.97, H 2.52, N 3.34. IR:  $\tilde{\nu}$  = 1501 (w), 1452 (w), 1439 (w), 1093 (w,  $\nu_{\text{ClO}_4^-}$ ), 1058 (m), 953 (m), 797 (s, C<sub>6</sub>F<sub>5</sub>, X-sensitive vibr.),<sup>[103]</sup> 622 (w,  $\nu_{\text{ClO}_4^-}$ ), 696 (w) cm<sup>-1</sup>.  $A_M$  (Me<sub>2</sub>CO) = 241.43  $\Omega^{-1}$  cm<sup>2</sup> mol<sup>-1</sup>. <sup>1</sup>H NMR ([D<sub>6</sub>]Me<sub>2</sub>CO, 295 K):  $\delta$  = 8.70 (dd, <sup>3</sup>J<sub>H<sub>2</sub>,H<sub>3</sub></sub> = 8.12 Hz, <sup>4</sup>J<sub>H<sub>2</sub>,H<sub>4</sub></sub> = 1.10 Hz, overlapped with H4, H2), 8.67 (m, overlapped with H2, H4), 8.02 (m, H-*p*-py), 8.15 (m, 4H-*o*-Ph), 7.90 (m, 2H-*m*-py), 7.88 (d, <sup>3</sup>J<sub>H<sub>5</sub>,H<sub>6</sub></sub> = 8.79 Hz, H5), 7.84 (d, <sup>3</sup>J<sub>H<sub>6</sub>,H<sub>5</sub></sub> = 8.85 Hz, H6), 7.63 (dd, <sup>3</sup>J<sub>H<sub>7</sub>,H<sub>8</sub></sub> = 7.97 Hz, <sup>4</sup>J<sub>H<sub>7</sub>,H<sub>9</sub></sub> = 0.54 Hz, H7), 7.49 (m, 4H-*m*-Ph and 2H-*p*-Ph), 7.24 (dd, <sup>3</sup>J<sub>H<sub>8</sub>,H<sub>7</sub></sub> = 7.62 Hz, <sup>3</sup>J<sub>H<sub>8</sub>,H<sub>9</sub></sub> = 7.45 Hz, H8), 6.89 (d, <sup>3</sup>J<sub>H<sub>9</sub>,H<sub>8</sub></sub> = 7.28 Hz, <sup>3</sup>J<sub>H<sub>9</sub>,Pt</sub> = 71.51 Hz, H9) ppm. <sup>19</sup>F NMR ([D<sub>6</sub>]Me<sub>2</sub>CO, 295 K):  $\delta$  = -118.26 (<sup>3</sup>J<sub>F,Pt</sub> = 505.91 Hz, *o*-F), -165.50 (*p*-F), -166.94 (*m*-F, br. m) ppm.

**[Pt(C<sub>6</sub>F<sub>5</sub>)(bzq)(tht)]<sub>2</sub>AgClO<sub>4</sub> (9):** Yield 0.200 g, 71%. C<sub>46</sub>H<sub>32</sub>AgClF<sub>10</sub>N<sub>2</sub>O<sub>4</sub>Pt<sub>2</sub>S<sub>2</sub> (1464.37): calcd. C 37.73, H 2.20, N 1.91, S 4.38; found C 37.29, H 2.01, N 1.92, S 3.89. IR:  $\tilde{\nu}$  = 1503 (m), 1453 (m), 1439 (m), 1269 (w,  $\nu_{\text{SC}}$ ), 1256 (w,  $\nu_{\text{SC}}$ ), 1086 (m,  $\nu_{\text{ClO}_4^-}$ ), 1061 (s), 952 (s), 801 (m, C<sub>6</sub>F<sub>5</sub>, X-sensitive vibr.),<sup>[103]</sup> 621 (w,  $\nu_{\text{ClO}_4^-}$ ) cm<sup>-1</sup>.  $A_M$  (Me<sub>2</sub>CO) = 238.73  $\Omega^{-1}$  cm<sup>2</sup> mol<sup>-1</sup>. <sup>1</sup>H NMR ([D<sub>6</sub>]acetone, 295 K):  $\delta$  = 9.26 (dd, <sup>3</sup>J<sub>H<sub>2</sub>,H<sub>3</sub></sub> = 5.24 Hz, <sup>4</sup>J<sub>H<sub>2</sub>,H<sub>4</sub></sub> = 1.27 Hz, <sup>3</sup>J<sub>H<sub>2</sub>,Pt</sub> = 21.9 Hz, H2), 8.77 (dd, <sup>3</sup>J<sub>H<sub>4</sub>,H<sub>3</sub></sub> = 8.10 Hz, <sup>4</sup>J<sub>H<sub>4</sub>,H<sub>2</sub></sub> = 1.21 Hz, H4), 7.93 (dd, <sup>3</sup>J<sub>H<sub>3</sub>,H<sub>4</sub></sub> = 8.08 Hz, <sup>3</sup>J<sub>H<sub>3</sub>,H<sub>2</sub></sub> = 5.23 Hz, H3), 7.91 (d, <sup>3</sup>J<sub>H<sub>5</sub>,H<sub>6</sub></sub> = 8.74 Hz, H5), 7.86 (d, <sup>3</sup>J<sub>H<sub>6</sub>,H<sub>5</sub></sub> = 8.77 Hz, H6), 7.73 (dd, <sup>3</sup>J<sub>H<sub>7</sub>,H<sub>8</sub></sub> = 8.00 Hz, <sup>4</sup>J<sub>H<sub>7</sub>,H<sub>9</sub></sub> = 0.70 Hz, H7), 7.34 (dd, <sup>3</sup>J<sub>H<sub>8</sub>,H<sub>9</sub></sub> = 7.89 Hz, <sup>3</sup>J<sub>H<sub>8</sub>,H<sub>7</sub></sub> = 7.20 Hz, H8), 6.86 (d, <sup>3</sup>J<sub>H<sub>9</sub>,H<sub>8</sub></sub> = 7.03 Hz, <sup>3</sup>J<sub>H<sub>9</sub>,Pt</sub> = 58.53 Hz, H9), 3.17 (m, 4H-*m*-tht), 1.86 (m, 4H-*o*-tht) ppm. <sup>19</sup>F NMR ([D<sub>6</sub>]Me<sub>2</sub>CO, 295 K):  $\delta$  = -117.47 (<sup>3</sup>J<sub>F,Pt</sub> = 506.05 Hz, *o*-F), -164.62 (*p*-F), -165.86 (*m*-F, br. m) ppm.

**Preparation of [Pt(C<sub>6</sub>F<sub>5</sub>)(bzq)(MeCN)]<sub>2</sub>AgClO<sub>4</sub> (10):** To a solution of [Pt(bzq)(C<sub>6</sub>F<sub>5</sub>)(MeCN)] (0.200 g, 0.344 mmol) in Me<sub>2</sub>CO (20 mL) at 0 °C and under an Ar atmosphere was added AgClO<sub>4</sub> (0.0357 g, 0.172 mmol). After 30 min of stirring in the absence of light, the solution was evaporated to dryness. The yellow residue was treated with *n*-hexane (10 mL), filtered, and finally air dried. Yield 0.211 g, 96%. C<sub>42</sub>H<sub>22</sub>AgClF<sub>10</sub>N<sub>4</sub>O<sub>4</sub>Pt<sub>2</sub> (1370.13): calcd. C 36.82, H 1.62, N 4.09; found C 37.17, H 2.02, N 3.73. IR:  $\tilde{\nu}$  = 2165 (vw,  $\nu_{\text{CN}}$ ), 1504 (m), 1443 (m), 1456 (m), 1060 (s), 1090 (m,  $\nu_{\text{ClO}_4^-}$ ), 953 (s), 804 (m, C<sub>6</sub>F<sub>5</sub>, X-sensitive vibr.),<sup>[103]</sup> 623 (m,  $\nu_{\text{ClO}_4^-}$ ) cm<sup>-1</sup>.  $A_M$  (Me<sub>2</sub>CO) = 225.67  $\Omega^{-1}$  cm<sup>2</sup> mol<sup>-1</sup>. <sup>1</sup>H NMR ([D<sub>6</sub>]Me<sub>2</sub>CO, 295 K):  $\delta$  = 9.17 (dd, <sup>3</sup>J<sub>H<sub>2</sub>,H<sub>3</sub></sub> = 5.13 Hz, <sup>3</sup>J<sub>H<sub>2</sub>,H<sub>4</sub></sub> = 1.06 Hz, <sup>3</sup>J<sub>H<sub>2</sub>,Pt</sub> = 24.70 Hz, H2), 8.73 (dd, <sup>3</sup>J<sub>H<sub>4</sub>,H<sub>3</sub></sub> = 8.18 Hz, <sup>4</sup>J<sub>H<sub>4</sub>,H<sub>2</sub></sub> = 1.03 Hz, H4), 7.89 (d, <sup>3</sup>J<sub>H<sub>5</sub>,H<sub>6</sub></sub> = 8.74 Hz, H5), 7.87 (m, overlapped with H5 and H6, H3), 7.84 (d, <sup>3</sup>J<sub>H<sub>6</sub>,H<sub>5</sub></sub> = 8.79 Hz, H6), 7.68 (d, <sup>3</sup>J<sub>H<sub>7</sub>,H<sub>8</sub></sub> = 7.95 Hz, H7), 7.27 (dd, <sup>3</sup>J<sub>H<sub>8</sub>,H<sub>7</sub></sub> = 7.75 Hz, <sup>3</sup>J<sub>H<sub>8</sub>,H<sub>9</sub></sub> = 7.69 Hz, H8), 6.95 (d, <sup>3</sup>J<sub>H<sub>9</sub>,H<sub>8</sub></sub> = 7.69 Hz, <sup>3</sup>J<sub>H<sub>9</sub>,Pt</sub> = 63.0 Hz, H9), 2.65 (s, H<sub>MeCN</sub>) ppm. <sup>19</sup>F NMR ([D<sub>6</sub>]Me<sub>2</sub>CO, 295 K):  $\delta$  = -117.87 (<sup>3</sup>J<sub>F,Pt</sub> = 492.0 Hz, *o*-F), -165.81 (*p*-F), -167.14 (*m*-F, br. m) ppm.

**Preparation of [Pt(C<sub>6</sub>F<sub>5</sub>)(bzq)(PPh<sub>3</sub>)Ag(pyPh<sub>2</sub>)]ClO<sub>4</sub> (11):** To a solution of [Pt(bzq)(C<sub>6</sub>F<sub>5</sub>)(pyPh<sub>2</sub>)] (0.200 g, 0.259 mmol) in Me<sub>2</sub>CO (20 mL) at 0 °C and under an Ar atmosphere was added [Ag(OClO<sub>3</sub>)(PPh<sub>3</sub>)] (0.121 g, 0.259 mmol). After 30 min of stirring in the absence of light, the solution was evaporated to dryness. The oily yellow residue was treated with *n*-hexane (10 mL) and allowed to stir for 60 min. After this time, the yellow solid formed was filtered off and air dried. Yield 0.263 g, 88%. C<sub>54</sub>H<sub>36</sub>AgClF<sub>5</sub>N<sub>2</sub>O<sub>4</sub>Pt (1241.25): calcd. C 52.25, H 2.92, N 2.26; found C 52.02, H 2.81, N 2.24. IR:  $\tilde{\nu}$  = 1501 (w), 1456 (w), 1435 (w), 1092 (m,  $\nu_{\text{ClO}_4^-}$ ), 1059 (w), 957 (w), 803 (w, C<sub>6</sub>F<sub>5</sub>, X-sensitive vibr.), 621 (w,  $\nu_{\text{ClO}_4^-}$ ), 693 (w), 531 (w), 512 (w) cm<sup>-1</sup>.  $A_M$  (Me<sub>2</sub>CO) = 246.87  $\Omega^{-1}$  cm<sup>2</sup> mol<sup>-1</sup>. <sup>1</sup>H NMR ([D<sub>6</sub>]Me<sub>2</sub>CO, 295 K):  $\delta$  = 8.64 (dd, <sup>3</sup>J<sub>H<sub>4</sub>,H<sub>3</sub></sub> = 8.07 Hz, <sup>3</sup>J<sub>H<sub>4</sub>,H<sub>2</sub></sub> = 1.0 Hz, H4), 8.34 (d, <sup>3</sup>J<sub>H<sub>2</sub>,H<sub>3</sub></sub> = 5.36 Hz, <sup>3</sup>J<sub>H<sub>2</sub>,Pt</sub> = 26.36 Hz, H2), 8.15 (m, 4H-*o*-Ph), 8.06 (m, H-*p*-py), 7.99 (d, <sup>3</sup>J<sub>H<sub>5</sub>,H<sub>6</sub></sub> = 8.74 Hz, H5), 7.91 (m, 2H-*m*-py), 7.85 (d, <sup>3</sup>J<sub>H<sub>6</sub>,H<sub>5</sub></sub> = 8.87 Hz, H6), 7.74 [m, H7 and H-*m*-Ph (PPh<sub>3</sub>)], 7.55–7.42 [m, H8 and 3H-*p*-Ph (PPh<sub>3</sub>), 6H-*o*-Ph (PPh<sub>3</sub>), 4H-*m*-Ph (PPh<sub>2</sub>), 2H-*p*-Ph (PPh<sub>2</sub>)], 7.32 (dd, <sup>3</sup>J<sub>H<sub>3</sub>,H<sub>4</sub></sub> = 8.06 Hz, <sup>4</sup>J<sub>H<sub>3</sub>,H<sub>2</sub></sub> = 5.38 Hz, H6), 7.13 (t, <sup>3</sup>J<sub>H<sub>9</sub>,H<sub>8</sub></sub> = 6.21 Hz, <sup>3</sup>J<sub>H<sub>2</sub>,Pt</sub> = 47.40 Hz, H9) ppm. <sup>19</sup>F NMR ([D<sub>6</sub>]Me<sub>2</sub>CO, 295 K):  $\delta$  = -116.93 (<sup>3</sup>J<sub>F,Pt</sub> = 500.65 Hz, *o*-F), 167.16 (*m*-F, br. m), -166.88 (*p*-F) ppm. <sup>31</sup>P NMR ([D<sub>6</sub>]Me<sub>2</sub>CO, 295 K):  $\delta$  = 26.59 (s,  $J_{\text{P,Pt}}$  = 2147.8 Hz) ppm.

**X-ray Structure Determinations:** Crystal data and other details of the structure analyses are presented in Tables 12 and 13. Suitable crystals for X-ray diffraction studies were obtained by slow diffusion of *n*-hexane into concentrated solutions of the complexes in CH<sub>2</sub>Cl<sub>2</sub> or Me<sub>2</sub>CO (3 mL). Crystals were mounted at the end of quartz fibers. The radiation used in all cases was graphite monochromated Mo- $K_{\alpha}$  ( $\lambda$  = 0.71073 Å). X-ray intensity data were collected with an Oxford Diffraction Xcalibur diffractometer. The diffraction frames were integrated and corrected from absorption by using the CrysAlis RED program.<sup>[104]</sup> The structures were solved by Patterson and Fourier methods and refined by full-matrix least-squares on  $F^2$  with SHELXL-97.<sup>[105]</sup> All non-hydrogen atoms were assigned anisotropic displacement parameters and refined without positional constraints, except as noted below. All hydrogen atoms were constrained to idealized geometries and assigned isotropic displacement parameters equal to 1.2 times the  $U_{\text{iso}}$  values of their attached parent atoms (1.5 times for the methyl hydrogen atoms). In the structure of **4**·2/3CH<sub>2</sub>Cl<sub>2</sub>, three complete complexes are found in the asymmetric unit. In two of them, the  $\beta$  CH<sub>2</sub> fragments of the tht ligands are disordered over two positions, which were refined with partial occupancy 0.60/0.40 and 0.65/0.35. Weak re-

Table 12. Crystal data and structure refinement for [Pt(C<sub>6</sub>F<sub>5</sub>)(bzq)(PPh<sub>3</sub>)]·0.2Me<sub>2</sub>CO (**2**·0.2Me<sub>2</sub>CO), [Pt(C<sub>6</sub>F<sub>5</sub>)(bzq)(tht)]·2/3CH<sub>2</sub>Cl<sub>2</sub> (**4**·2/3CH<sub>2</sub>Cl<sub>2</sub>), and [Pt(C<sub>6</sub>F<sub>5</sub>)(bzq)(MeCN)] (**5**).

	2·0.2Me <sub>2</sub> CO	4·2/3CH <sub>2</sub> Cl <sub>2</sub>	5
Formula	C <sub>37</sub> H <sub>23</sub> F <sub>5</sub> NP <sub>3</sub> Pt·0.2Me <sub>2</sub> CO	C <sub>23</sub> H <sub>16</sub> F <sub>5</sub> NPtS·2/3CH <sub>2</sub> Cl <sub>2</sub>	C <sub>21</sub> H <sub>11</sub> F <sub>5</sub> N <sub>2</sub> Pt
Formula weight	814.24	685.14	581.41
Crystal system	triclinic	monoclinic	monoclinic
Space group	<i>P</i> $\bar{1}$	<i>Pc</i>	<i>P2</i> <sub>1</sub> / <i>c</i>
<i>a</i> [Å]	14.3213(3)	16.1169(3)	13.851(2)
<i>b</i> [Å]	14.7249(4)	12.4389(2)	7.4016(7)
<i>c</i> [Å]	16.0887(5)	16.4671(3)	17.653(2)
$\alpha$ [°]	80.101(3)	90	90
$\beta$ [°]	79.902(2)	93.036(2)	108.066(14)
$\gamma$ [°]	66.437(2)	90	90
<i>V</i> [Å <sup>3</sup> ]	3042.17(14)	3296.63(10)	12406.2(7)
<i>Z</i>	4	6	4
<i>D<sub>c</sub></i> [g cm <sup>-3</sup> ]	1.778	2.071	2.245
<i>T</i> [K]	100(1)	100(1)	100(1)
$\mu$ (Mo-K $\alpha$ ) [mm <sup>-1</sup> ]	4.726	6.697	8.217
<i>F</i> (000)	1586	1968	1096
$\theta$ range [°]	4.2–26.0	4.2–28.9	4.1–25.5
Reflections collected	28562	34078	11311
Independent reflections	11905	14799	3170
<i>R</i> <sub>int</sub>	0.0292	0.0425	0.0601
<i>R</i> <sub>1</sub> , <i>wR</i> <sub>2</sub> <sup>[a]</sup> [ <i>I</i> > 2 $\sigma$ ( <i>I</i> )]	0.0426, 0.0826	0.0364, 0.0908	0.0416, 0.0988
<i>R</i> <sub>1</sub> , <i>wR</i> <sub>2</sub> <sup>[a]</sup> (all data)	0.0536, 0.0849	0.0413, 0.0926	0.0525, 0.1026
GOF ( <i>F</i> <sup>2</sup> ) <sup>[b]</sup>	1.122	1.030	1.030
Absolute structure par.	–	0.020(5)	–

[a]  $R_1 = \Sigma(|F_o| - |F_c|)/\Sigma|F_o|$ ,  $wR_2 = [\Sigma w(F_o^2 - F_c^2)^2/\Sigma w(F_o^2)]^{1/2}$ .

[b] Goodness-of-fit =  $[\Sigma w(F_o^2 - F_c^2)^2/(n_{\text{obsd.}} - n_{\text{param.}})]^{1/2}$ .

straints were applied in the interatomic C–C distances and thermal parameters of these fragments. For **10**·2.5CH<sub>2</sub>Cl<sub>2</sub>·0.5*n*-C<sub>6</sub>H<sub>14</sub>, restraints were used in some structural and thermal parameters of the C atoms of the bzq ligands. Very diffuse solvent was found during the refinement stages and was modeled as several CH<sub>2</sub>Cl<sub>2</sub> moieties, some of them disordered, with a total occupancy of 2.5, and half of an *n*-hexane molecule. Restraints were used in the structural and thermal parameters of these units.

Full-matrix least-squares refinement of these models against *F*<sup>2</sup> converged to final residual indices given in Tables 12 and 13. CCDC-906692 (for **2**), -906693 (for **4**), -906694 (for **5**), -906695 (for **7**), -906696 (for **9**), -906697 (for **10**), and -906698 (for **11**) contain the supplementary crystallographic data for this paper. These data can be obtained free of charge from The Cambridge Crystallographic Data Centre via www.ccdc.cam.ac.uk/data\_request/cif.

**Computational Methods:** DFT calculations were performed by using the hybrid functionals B3LYP<sup>[106,107]</sup> for complexes **2**, **4**, and **5** and M06<sup>[108]</sup> for complexes **9**, **10**, and **11**Me under the Gaussian 09 package.<sup>[109]</sup> The SDD pseudopotential and associated basis set<sup>[110]</sup> was used for platinum and silver atoms, and the 6-31G(d)<sup>[111,112]</sup> basis set was used for all other atoms. Geometry optimizations were performed under no symmetry restrictions by using initial coordinates derived from X-ray data of the same or comparable complexes. Frequency calculations were used to confirm the stationary points were true minima. TD-DFT calculations were performed by using the polarized continuum model approach implemented in the Gaussian 09 software. A Mulliken population analysis was included for interpretation purposes. Molecular orbitals were visualized by using the Molekel program package.<sup>[113]</sup>

**Supporting Information** (see footnote on the first page of this article): Absorption data of solutions of **1–11** at room temperature;

Table 13. Crystal data and structure refinement for [{Pt(C<sub>6</sub>F<sub>5</sub>)(bzq)(PPh<sub>3</sub>)<sub>2</sub>Ag]ClO<sub>4</sub>·CH<sub>2</sub>Cl<sub>2</sub> (**7**·CH<sub>2</sub>Cl<sub>2</sub>), [{Pt(C<sub>6</sub>F<sub>5</sub>)(bzq)(tht)<sub>2</sub>Ag]ClO<sub>4</sub>·1.5Me<sub>2</sub>CO (**9**·1.5Me<sub>2</sub>CO), [{Pt(C<sub>6</sub>F<sub>5</sub>)(bzq)(MeCN)<sub>2</sub>Ag]ClO<sub>4</sub>·2.5CH<sub>2</sub>Cl<sub>2</sub>·0.5*n*-C<sub>6</sub>H<sub>14</sub> (**10**·2.5CH<sub>2</sub>Cl<sub>2</sub>·0.5*n*-C<sub>6</sub>H<sub>14</sub>), and [(C<sub>6</sub>F<sub>5</sub>)(bzq)(PPh<sub>3</sub>)Pt(pyPh<sub>2</sub>)]ClO<sub>4</sub>·CH<sub>2</sub>Cl<sub>2</sub> (**11**·CH<sub>2</sub>Cl<sub>2</sub>).

	7·CH <sub>2</sub> Cl <sub>2</sub>	9·1.5Me <sub>2</sub> CO	10·2.5CH <sub>2</sub> Cl <sub>2</sub> ·0.5 <i>n</i> -C <sub>6</sub> H <sub>14</sub>	11·CH <sub>2</sub> Cl <sub>2</sub>
Formula	C <sub>74</sub> H <sub>46</sub> AgClF <sub>10</sub> N <sub>2</sub> O <sub>4</sub> P <sub>2</sub> Pt <sub>2</sub> ·CH <sub>2</sub> Cl <sub>2</sub>	C <sub>46</sub> H <sub>32</sub> AgClF <sub>10</sub> N <sub>2</sub> O <sub>4</sub> Pt <sub>2</sub> S <sub>2</sub> ·1.5Me <sub>2</sub> CO	C <sub>42</sub> H <sub>22</sub> AgClF <sub>10</sub> N <sub>4</sub> O <sub>4</sub> Pt <sub>2</sub> ·2.5CH <sub>2</sub> Cl <sub>2</sub> ·0.5 <i>n</i> -C <sub>6</sub> H <sub>14</sub>	C <sub>54</sub> H <sub>36</sub> AgClF <sub>5</sub> N <sub>2</sub> O <sub>4</sub> PPt·CH <sub>2</sub> Cl <sub>2</sub>
<i>M<sub>t</sub></i>	1897.49	1551.47	1625.54	1326.15
Crystal system	monoclinic	triclinic	triclinic	triclinic
Space group	<i>P2</i> <sub>1</sub> / <i>c</i>	<i>P</i> $\bar{1}$	<i>P</i> $\bar{1}$	<i>P</i> $\bar{1}$
<i>a</i> [Å]	13.1438(2)	13.5673(8)	13.9756(4)	13.4888(2)
<i>b</i> [Å]	35.7903(8)	14.4385(11)	14.3662(3)	13.5126(2)
<i>c</i> [Å]	14.3105(3)	15.3982(8)	16.1823(3)	14.6245(2)
$\alpha$ [°]	90	72.599(6)	79.6218(17)	106.249(1)
$\beta$ [°]	102.9667(19)	68.987(5)	69.783(2)	107.091(1)
$\gamma$ [°]	90	64.745(7)	64.539(2)	90.684(1)
<i>V</i> [Å <sup>3</sup> ]	6560.3(2)	2508.2(3)	2750.84(11)	2433.18(6)
<i>Z</i>	4	2	2	2
<i>D<sub>c</sub></i> [g cm <sup>-3</sup> ]	1.921	2.052	1.963	1.810
<i>T</i> [K]	100(1)	100(1)	100(1)	100(1)
$\mu$ [mm <sup>-1</sup> ]	4.804	6.175	5.796	3.542
<i>F</i> (000)	3672	1485	1548	1300
$\theta$ range [°]	4.2–28.9	4.3–28.9	4.1–28.9	4.2–35.3
Reflections collected	57416	49929	58605	91933
Independent reflections	15626	11819	13069	18524
<i>R</i> <sub>int</sub>	0.0427	0.0600	0.0624	0.0286
<i>R</i> <sub>1</sub> , <i>wR</i> <sub>2</sub> <sup>[a]</sup> [ <i>I</i> > 2 $\sigma$ ( <i>I</i> )]	0.0347, 0.0566	0.0395, 0.0997	0.0571, 0.1524	0.0190, 0.0419
<i>R</i> <sub>1</sub> , <i>wR</i> <sub>2</sub> <sup>[a]</sup> (all data)	0.0531, 0.0586	0.0569, 0.1070	0.0942, 0.1646	0.0244, 0.0425
GOF ( <i>F</i> <sup>2</sup> ) <sup>[b]</sup>	1.008	1.044	1.030	1.027

[a]  $R_1 = \Sigma(|F_o| - |F_c|)/\Sigma|F_o|$ ,  $wR_2 = [\Sigma w(F_o^2 - F_c^2)^2/\Sigma w(F_o^2)]^{1/2}$ . [b] Goodness-of-fit =  $[\Sigma w(F_o^2 - F_c^2)^2/(n_{\text{obsd.}} - n_{\text{param.}})]^{1/2}$ .

DFT-optimized coordinates and selected singlet excited states calculated by TD-DFT for complexes **2**, **4**, **5**, **9**, **10**, and **11Me** in CH<sub>2</sub>Cl<sub>2</sub>; emission data of solutions of **1–5** at 77 K; views of the supramolecular arrangement showing  $\pi\cdots\pi$  stacking for complexes **2** and **5**; normalized absorption spectra of **2** in solutions of different solvents at room temperature; energy levels and electron-density diagrams of the frontier molecular orbitals involved in the lower-energy excited calculated states for **4**, **5**, **9**, and **10**; normalized DRUV spectra of complexes **1–5** in the solid state; and normalized emission and excitation spectra of **5** and **10** in the solid state.

## Acknowledgments

This work was supported by the Spanish Ministerio de Ciencia e Innovación (MICINN) (DGPTC/FEDER) (project number CTQ2008-06669-C02-01/BQU). The authors thank Mariano Perálvarez (IREC) for the QY measurements. We thank CESGA (Supercomputing Centre of Galicia, Santiago de Compostela, Spain) for the supercomputing facilities.

- [1] P. Pykkö, *Chem. Rev.* **1997**, *97*, 597.
- [2] P. Pykkö, *Angew. Chem.* **2004**, *116*, 4512; *Angew. Chem. Int. Ed.* **2004**, *43*, 4412.
- [3] L. H. Gade, *Angew. Chem.* **2001**, *113*, 3685; *Angew. Chem. Int. Ed.* **2001**, *40*, 3573.
- [4] M. A. Carvajal, S. Álvarez, J. J. Novoa, *Chem. Eur. J.* **2004**, *10*, 2117.
- [5] A. Díez, E. Lalinde, M. T. Moreno, *Coord. Chem. Rev.* **2011**, *255*, 2426.
- [6] E. J. Fernández, A. Laguna, J. M. López de Luzuriaga, *Dalton Trans.* **2007**, 1969.
- [7] E. J. Fernández, A. Laguna, J. M. López de Luzuriaga, *Coord. Chem. Rev.* **2005**, *249*, 1423.
- [8] A. Laguna (Ed.), *Modern Supramolecular Gold Chemistry*, Wiley-VCH, Weinheim, **2008**.
- [9] E. J. Fernández, J. M. López de Luzuriaga, M. Monge, M. A. Rodríguez, O. Crespo, M. C. Gimeno, A. Laguna, P. G. Jones, *Chem. Eur. J.* **2000**, *6*, 636.
- [10] V. W. W. Yam, E. C. C. Cheng, *Chem. Soc. Rev.* **2008**, *37*, 1806.
- [11] H. Schmidbaur, A. Schier, *Chem. Soc. Rev.* **2008**, *37*, 1931.
- [12] S. Sculfort, P. Braunstein, *Chem. Soc. Rev.* **2011**, *40*, 2741.
- [13] J. Forniés, A. Martín in *Metal Clusters in Chemistry* (Eds.: P. Braunstein, L. A. Oro, P. R. Raithby), Wiley-VCH, Weinheim, **1999**, vol. 1, pp. 417.
- [14] J. Forniés, C. Fortuño, S. Ibáñez, A. Martín, *Inorg. Chem.* **2008**, *47*, 5978.
- [15] J. Forniés, S. Fuertes, A. Martín, V. Sicilia, B. Gil, E. Lalinde, *Dalton Trans.* **2009**, 2224.
- [16] J. Forniés, S. Ibáñez, A. Martín, B. Gil, E. Lalinde, M. T. Moreno, *Organometallics* **2004**, *23*, 3963.
- [17] J. Forniés, S. Ibáñez, A. Martín, M. Sanz, J. R. Berenguer, E. Lalinde, J. Torroba, *Organometallics* **2006**, *25*, 4331.
- [18] J. R. Berenguer, A. Díez, J. Fernández, J. Forniés, A. García, B. Gil, E. Lalinde, M. T. Moreno, *Inorg. Chem.* **2008**, *47*, 7703.
- [19] J. M. Casas, J. Forniés, S. Fuertes, A. Martín, V. Sicilia, *Organometallics* **2007**, *26*, 1674.
- [20] W. Chen, F. Liu, T. Nishioka, K. Matsumoto, *Eur. J. Inorg. Chem.* **2003**, 4234.
- [21] A. Díez, J. Forniés, J. Gómez, E. Lalinde, A. Martín, M. T. Moreno, S. Sánchez, *Dalton Trans.* **2007**, 3653.
- [22] T. Yamaguchi, F. Yamazaki, T. Ito, *J. Am. Chem. Soc.* **1999**, *121*, 7405.
- [23] T. Yamaguchi, F. Yamazaki, T. Ito, *J. Am. Chem. Soc.* **2001**, *123*, 743.
- [24] M.-E. Moret, P. Chen, *J. Am. Chem. Soc.* **2009**, *131*, 5675.
- [25] G. Kampf, P. J. S. Miguel, M. Willermann, A. Schneider, B. Lippert, *Chem. Eur. J.* **2008**, *14*, 6882.
- [26] D. E. Janzen, L. F. Mehne, D. G. VanDerveer, G. J. Grant, *Inorg. Chem.* **2005**, *44*, 8182.
- [27] S. A. Baudron, M. W. Hosseini, *Chem. Commun.* **2008**, 4558.
- [28] G.-Q. Yin, Q.-H. Wei, L.-Y. Zhang, Z.-N. Chen, *Organometallics* **2006**, *25*, 580.
- [29] M.-E. Moret, P. Chen, *Organometallics* **2008**, *27*, 4903.
- [30] L. R. Falvello, J. Forniés, R. Garde, A. García, E. Lalinde, M. T. Moreno, A. Steiner, M. Tomás, I. Usón, *Inorg. Chem.* **2006**, *45*, 2543.
- [31] O. Crespo, A. Laguna, E. J. Fernández, J. M. López de Luzuriaga, P. G. Jones, M. Teichert, M. Monge, P. Pykkö, N. Runeberg, M. Schütz, H. J. Werner, *Inorg. Chem.* **2000**, *39*, 4786.
- [32] S. Fuertes, C. H. Woodall, P. R. Raithby, V. Sicilia, *Organometallics* **2012**, *31*, 4228.
- [33] L. R. Falvello, J. Forniés, A. Martín, V. Sicilia, P. Villarroya, *Organometallics* **2002**, *21*, 4604.
- [34] E. Alonso, J. Forniés, C. Fortuño, A. Martín, A. G. Orpen, *Organometallics* **2003**, *22*, 5011.
- [35] F. D. Rochon, R. Melanson, *Acta Crystallogr., Sect. C: Cryst. Struct. Commun.* **1988**, *44*, 474.
- [36] L. R. Falvello, J. Forniés, C. Fortuño, F. Durán, A. Martín, *Organometallics* **2002**, *21*, 2226.
- [37] I. Ara, L. R. Falvello, J. Forniés, J. Gómez, E. Lalinde, R. I. Merino, I. Usón, *J. Organomet. Chem.* **2002**, *663*, 284.
- [38] L. R. Falvello, J. Forniés, E. Lalinde, B. Menjón, M. A. García Monforte, M. T. Moreno, M. Tomás, *Chem. Commun.* **2007**, 3838.
- [39] J. Forniés, S. Ibáñez, E. Lalinde, A. Martín, M. T. Moreno, A. C. Tsipis, *Dalton Trans.* **2012**, *41*, 3439.
- [40] P. T. Chou, Y. Chi, *Chem. Eur. J.* **2007**, *13*, 380.
- [41] M. W. Cooke, G. S. Hanan, *Chem. Soc. Rev.* **2007**, *36*, 1466.
- [42] R. C. Evans, P. Douglas, C. J. Wiscom, *Coord. Chem. Rev.* **2006**, *250*, 2093.
- [43] E. Holder, B. M. W. Langeveld, U. S. Schubert, *Adv. Mater.* **2005**, *17*, 1109.
- [44] M. D. McClenaghan, N. D. Leydet, Y. Maubert, M. T. Indelli, S. Campagna, *Coord. Chem. Rev.* **2005**, *249*, 1336.
- [45] S. S. Sun, A. J. Lees, *Coord. Chem. Rev.* **2002**, *230*, 171.
- [46] W. Y. Wong, *Comments Inorg. Chem.* **2005**, *26*, 39.
- [47] M. H. V. Huynh, D. M. Dattelbaum, T. J. Meyer, *Coord. Chem. Rev.* **2005**, *249*, 457.
- [48] A. Vogler, H. Kunkely, *Top. Curr. Chem.* **2001**, *213*, 143.
- [49] P. Thanasekaran, R. T. Liao, Y. H. Liu, T. Rajendran, S. Rajagopal, K. L. Lu, *Coord. Chem. Rev.* **2005**, *249*, 1085.
- [50] Special issue on the "Thirteenth International Symposium on Photochemistry and Photophysics of Coordination Compounds (ISPPCC)": *Coord. Chem. Rev.* **2000**, 208.
- [51] B. Ma, P. I. Djurovich, M. E. Thompson, *Coord. Chem. Rev.* **2005**, *249*, 1501.
- [52] S. Pérez, C. López, A. Caubet, R. Bosque, X. Solans, M. F. Bardía, A. Roig, E. Molins, *Organometallics* **2004**, *23*, 224.
- [53] J. Forniés, V. Sicilia, J. M. Casas, A. Martín, J. A. López, C. Larraz, P. Borja, C. Ovejero, *Dalton Trans.* **2011**, *40*, 2898.
- [54] R. Usón, J. Forniés, M. Tomás, I. Ara, J. M. Casas, A. Martín, *J. Chem. Soc., Dalton Trans.* **1991**, 2253.
- [55] L. R. Falvello, J. Forniés, A. Martín, V. Sicilia, P. Villarroya, *Organometallics* **2002**, *21*, 4604.
- [56] I. Ara, J. Forniés, V. Sicilia, P. Villarroya, *Dalton Trans.* **2003**, 4238.
- [57] J. R. Berenguer, B. Gil, J. Fernández, J. Forniés, E. Lalinde, *Inorg. Chem.* **2009**, *48*, 5250.
- [58] C. Mealli, F. Pichierri, L. Randaccio, E. Zangrando, M. Krumm, D. Holtenrich, B. Lippert, *Inorg. Chem.* **1995**, *34*, 3418.
- [59] G. Aullón, S. Álvarez, *Inorg. Chem.* **1996**, *35*, 3137.
- [60] J. R. Berenguer, E. Lalinde, M. T. Moreno, S. Sánchez, J. Torroba, *Inorg. Chem.* **2012**, *51*, 11665.
- [61] J. Forniés, J. Gómez, E. Lalinde, M. T. Moreno, *Inorg. Chem.* **2001**, *40*, 5415.

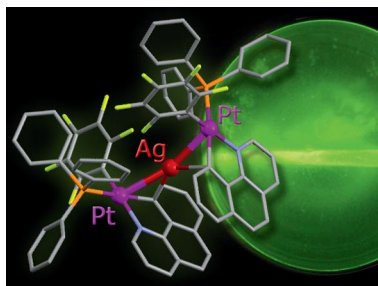
- [62] S. Fuertes, S. K. Brayshaw, P. R. Raithby, S. Schiffers, M. R. Warren, *Organometallics* **2012**, *31*, 105.
- [63] C. A. Hunter, J. K. M. Sanders, *J. Am. Chem. Soc.* **1990**, *112*, 5525.
- [64] C. A. Hunter, *Chem. Soc. Rev.* **1994**, *23*, 101.
- [65] A. Diez, J. Forniés, A. García, E. Lalinde, M. T. Moreno, *Inorg. Chem.* **2005**, *44*, 2443.
- [66] W. Lu, M. C. W. Chan, N. Zhu, C. M. Che, C. Li, Z. Hui, *J. Am. Chem. Soc.* **2004**, *126*, 7639.
- [67] V. W. Yam, R. P. L. Tang, K. M. C. Wong, X. X. Lu, K. K. Cheung, N. Zhu, *Chem. Eur. J.* **2002**, *8*, 4066.
- [68] S. J. Farley, D. L. Rochester, A. L. Thompson, J. A. K. Howard, J. A. Williams, *Inorg. Chem.* **2005**, *44*, 9690.
- [69] M. Munakata, L. P. Wu, G. L. Ning, T. Kuroda-Sowa, M. Maekawa, Y. Suenaga, N. Maeno, *J. Am. Chem. Soc.* **1999**, *121*, 4968.
- [70] M. Munakata, L. P. Wu, T. Kuroda-Sowa, M. Maekawa, Y. Suenaga, G. L. Ning, T. Kojima, *J. Am. Chem. Soc.* **1998**, *120*, 8610.
- [71] M. Munakata, J. C. Zhong, T. Kuroda-Sowa, M. Maekawa, Y. Suenaga, M. Kasahara, H. Konaka, *Inorg. Chem.* **2001**, *40*, 7087.
- [72] M. Munakata, L. P. Wu, T. Kuroda-Sowa, M. Maekawa, Y. Suenaga, T. Ohta, H. Konaka, *Inorg. Chem.* **2003**, *42*, 2553.
- [73] W.-B. Yuan, R.-D. Yang, L. Tan, *Transition Met. Chem.* **2004**, *29*, 380.
- [74] F. A. Cotton, L. R. Falvello, R. Usón, J. Forniés, M. Tomás, J. M. Casas, I. Ara, *Inorg. Chem.* **1987**, *26*, 1366.
- [75] R. Usón, J. Forniés, M. Tomás, J. M. Casas, F. A. Cotton, L. R. Falvello, R. Llusar, *Organometallics* **1988**, *7*, 2279.
- [76] R. Usón, J. Forniés, M. Tomás, J. M. Casas, *Angew. Chem.* **1989**, *101*, 782; *Angew. Chem. Int. Ed. Engl.* **1989**, *28*, 748.
- [77] J. Forniés, R. Navarro, M. Tomás, E. P. Urriolabeitia, *Organometallics* **1993**, *12*, 940.
- [78] J. M. Casas, L. R. Falvello, J. Forniés, A. Martín, *Inorg. Chem.* **1996**, *35*, 7867.
- [79] R. Usón, J. Forniés, L. R. Falvello, M. Tomás, J. M. Casas, A. Martín, *Inorg. Chem.* **1993**, *32*, 5212.
- [80] A. Martín, A. G. Orpen, *J. Am. Chem. Soc.* **1996**, *118*, 1464.
- [81] J. C. Zhong, M. Munakata, T. Kuroda-Sowa, M. Maekawa, Y. Suenaga, H. Konaka, *Inorg. Chem.* **2001**, *40*, 3191.
- [82] M. Wen, M. Maekawa, M. Munakata, Y. Suenaga, T. Kuroda-Sowa, *Inorg. Chim. Acta* **2002**, *338*, 111.
- [83] S. Q. Liu, T. Kuroda-Sowa, H. Konaka, Y. Suenaga, M. Maekawa, T. Mizutani, G. L. Ning, M. Munakata, *Inorg. Chem.* **2005**, *44*, 1031.
- [84] Y.-B. Dong, Y. Geng, J.-P. Ma, R.-Q. Huang, *Inorg. Chem.* **2005**, *44*, 1693.
- [85] Y.-B. Dong, G.-X. Jin, X. Zhao, B. Tang, R.-Q. Huang, M. D. Smith, K. E. Stitzer, H.-C. zur Loye, *Organometallics* **2004**, *23*, 1604.
- [86] Y.-B. Dong, X. Zhao, G.-X. Jin, R.-Q. Huang, M. D. Smith, *Eur. J. Inorg. Chem.* **2003**, 4017.
- [87] T. Brasey, A. Buryak, R. Scopelliti, K. Severin, *Eur. J. Inorg. Chem.* **2004**, 964.
- [88] M. Munakata, L. P. Wu, G. L. Ning, *Coord. Chem. Rev.* **2000**, *198*, 171.
- [89] A. P. Côté, G. K. H. Shimizu, *Inorg. Chem.* **2004**, *43*, 6663.
- [90] X.-M. Lin, Y. Ying, L. Chen, H.-C. Fang, Z.-Y. Zhou, Q.-G. Zhan, Y.-P. Cai, *Inorg. Chem. Commun.* **2009**, *12*, 316.
- [91] R. M. Hellyer, D. S. Larsen, S. Brooker, *Eur. J. Inorg. Chem.* **2009**, 1162.
- [92] L.-C. Song, G.-X. Jin, L.-Q. Zhao, H.-T. Wang, W.-X. Zhang, Q.-M. Hu, *Eur. J. Inorg. Chem.* **2009**, 419.
- [93] R. P. Feazell, C. E. Carson, K. K. Klausmeyer, *Inorg. Chem.* **2006**, *45*, 935.
- [94] N. Sadhukhan, S. K. Patra, K. Sana, J. K. Bera, *Organometallics* **2006**, *25*, 2914.
- [95] M. A. M. Abu-Youssef, R. Dey, Y. Gohar, A. a. A. Massoud, L. Öhrström, V. Langer, *Inorg. Chem.* **2007**, *46*, 5893.
- [96] A. Diez, J. Forniés, S. Fuertes, E. Lalinde, C. Larraz, J. A. López, A. Martín, M. T. Moreno, V. Sicilia, *Organometallics* **2009**, *28*, 1705.
- [97] A. Diez, J. Forniés, C. Larraz, E. Lalinde, J. A. López, A. Martín, M. T. Moreno, V. Sicilia, *Inorg. Chem.* **2010**, *49*, 3239.
- [98] F. M. Hwang, H. Y. Chen, P. S. Chen, C. S. Liu, Y. Chi, C. F. Shu, F. L. Wu, P. T. Chou, S. M. Peng, G. H. Lee, *Inorg. Chem.* **2005**, *44*, 1344.
- [99] J. Brooks, Y. Babayan, S. Lamansky, P. I. Djurovich, I. Tsyba, K. Bau, M. E. Thompson, *Inorg. Chem.* **2002**, *41*, 3055.
- [100] S. D. Cummings, R. Eisenberg, *J. Am. Chem. Soc.* **1996**, *118*, 1949.
- [101] J. A. G. Williams, *Chem. Soc. Rev.* **2009**, *38*, 1783.
- [102] J. A. G. Williams, *Top. Curr. Chem.* **2007**, *281*, 205.
- [103] E. J. Maslowsky, *Vibrational Spectra of Organometallic Compounds*, Wiley, New York, **1977**.
- [104] *CrysAlis, RED Program for X-ray CCD Camera Data Reduction*, Oxford Diffraction, Oxford, UK, **2004**.
- [105] G. M. Sheldrick, *SHELXL-97, Program for Crystal Structure Refinement*, University of Göttingen, Germany, **1997**.
- [106] A. D. Becke, *J. Chem. Phys.* **1993**, *98*, 5648.
- [107] C. T. Lee, W. T. Yang, R. G. Parr, *Phys. Rev. B* **1988**, *37*, 785.
- [108] Y. Zhao, D. G. Truhlar, *Theor. Chem. Acc.* **2008**, *120*, 215.
- [109] M. J. Frisch, G. W. Trucks, H. B. Schlegel, G. E. Scuseria, M. A. Robb, J. R. Cheeseman, G. Scalmani, V. Barone, B. Mennucci, G. A. Petersson, H. Nakatsuji, M. Caricato, X. Li, H. P. Hratchian, A. F. Izmaylov, J. Bloino, G. Zheng, J. L. Sonnenberg, M. Hada, M. Ehara, K. Toyota, R. Fukuda, J. Hasegawa, M. Ishida, T. Nakajima, Y. Honda, O. Kitao, H. Nakai, T. Vreven, J. A. Montgomery Jr., J. E. Peralta, F. Ogliaro, M. Bearpark, J. J. Heyd, E. Brothers, K. N. Kudin, V. N. Staroverov, R. Kobayashi, J. Normand, K. Raghavachari, A. Rendell, J. C. Burant, S. S. Iyengar, J. Tomasi, M. Cossi, N. Rega, J. M. Millam, M. Klene, J. E. Knox, J. B. Cross, V. Bakken, C. Adamo, J. Jaramillo, R. Gomperts, R. E. Stratmann, O. Yazyev, A. J. Austin, R. Cammi, C. Pomelli, J. W. Ochterski, R. L. Martin, K. Morokuma, V. G. Zakrzewski, G. A. Voth, P. Salvador, J. J. Dannenberg, S. Dapprich, A. D. Daniels, Ö. Farkas, J. B. Foresman, J. V. Ortiz, J. Cioslowski, D. J. Fox, *Gaussian 09*, Revision A.02, Gaussian, Inc., Wallingford, CT, **2009**.
- [110] D. Andrae, U. Häussermann, M. Dolg, H. Stoll, H. Preuss, *Theor. Chim. Acta* **1990**, *77*, 123.
- [111] R. Ditchfield, W. J. Herhe, J. A. Pople, *J. Chem. Phys.* **1971**, *54*, 724.
- [112] P. C. Hariharan, J. A. Pople, *Theor. Chim. Acta* **1973**, *28*, 213.
- [113] U. Varetto, *MOLEKEL*, v. 5.4, Swiss National Supercomputing Centre, Lugano, Switzerland, **2009**.

Received: December 18, 2012

Published Online: ■

## Pt–Ag Clusters

Trimetallic  $[\{Pt(C_6F_5)(bzq)L\}_2Ag]^+$  and bimetallic  $[(C_6F_5)(bzq)(PPh_3)PtAg(pyPh_2)]^+$  clusters containing Pt–Ag bonds were prepared from  $[Pt(C_6F_5)(bzq)L]$  ( $bzq = 7,8$ -benzoquinolate). These complexes have luminescent properties that were studied and interpreted with the help of time-dependent DFT calculations.



A. Martín,\* Ú. Belío, S. Fuertes,  
V. Sicilia ..... 1–18

Luminescent Pt–Ag Clusters Based on Neutral Benzoquinolate Cyclometalated Platinum Complexes 

**Keywords:** Donor–acceptor systems / Heterometallic complexes / Cluster compounds / Silver / Platinum / Luminescence / Metal–metal interactions / Pi interactions / Density functional calculations